# Exploring center strings in $SU(2)$ and $SU(3)$ relativistic Yang-Mills-Higgs models

L. E. Oxman[1] and D. Vercauteren[2,3]

[1]*Instituto de Física, Universidade Federal Fluminense, Campus da Praia Vermelha,*
*Niterói, 24210-340 Rio de Janeiro, Brazil*
[2]*Departamento de Física Teórica, Instituto de Física, Universidade do Estado do Rio de Janeiro,*
*Rua São Francisco Xavier 524, 20550-013 Maracanã, Rio de Janeiro, Brazil*
[3]*Duy Tân University, Institute of Research and Development,*
*P809, K7/25 Quang Trung, 550000 Hải Châu, Đà Nẵng, Vietnam*

We develop numerical tools and apply them to solve the relativistic Yang-Mills-Higgs equations in a model where the $SU(N)$ symmetry is spontaneously broken to its center. In $SU(2)$ and $SU(3)$, we obtain the different field profiles for infinite and finite center strings, with end points at external monopole sources. Exploration of parameter space permits the detection of a region where the equations get Abelianized. Finally, a general parametrization of the color structure of $SU(2)$ fields leads us to a reference point where an Abelian-like Bogomol'nyi-Prasad-Sommereld (BPS) bound is reconciled with $N$-ality.

## I. INTRODUCTION

Over the years, many lattice studies have been oriented toward obtaining the static potential from the Wilson loop average in pure Yang-Mills (YM) theories, for quarks in different representations. Asymptotic linearity [1], string-like behavior [2], and $N$-ality at asymptotic distances [3] are among the observed properties. The third one refers to the fact that string tensions depend on how the center $Z(N)$ is realized in a given $SU(N)$ quark representation.

Based on the idea of dual superconductivity [4–6], these properties have been explored by means of lattice calculations and effective models in a Higgs phase. In the former, the possibility to capture the path-integral measure by quantum ensembles of magnetic configurations is analyzed (see [7–16], and references therein). In the latter, phenomenological dimensionful scales are introduced from the beginning, proposing a dual superconductor where the confining string is a smooth vortex solution to the classical equations of motion. This is a magnetic object in the dual description that is supposed to effectively represent the chromoelectric confining string. The detailed knowledge we have about interquark lattice potentials, for different groups and representations, makes us wonder what the natural dual superconductor could be. In this context, gauge models with the $SU(N) \to Z(N)$ spontaneous symmetry breaking (SSB) pattern have been considered (see Refs. [17–22], and references therein). In this case, the manifold of vacua is the coset $\mathcal{M} = SU(N)/Z(N) = Ad(SU(N))$ [the adjoint representation of $SU(N)$], whose first homotopy group is $\Pi_1(\mathcal{M}) = Z(N)$. Then, the confining string would be represented by a smooth *center vortex*, hereafter referred to as a "center string" to avoid confusion with the center vortices in pure YM ensembles.

This SSB scenario is attractive because it naturally leads to $N$-ality (see the discussion in [21,22], and in Sec. V B).

With these ideas in mind, the initial objective of this work is to look for and test appropriate numerical methods to solve the center string field equations. These tools will permit one, in a forthcoming work, to contrast different proposals with existing lattice data obtained from Monte Carlo simulations. A part of the data could be used to adjust the parameters, and then we could make predictions to be compared with other data. This type of analysis has already been considered in Refs. [23–29]. In Refs. [26–28], an Abelian Higgs model that essentially describes a condensate of Abelian monopoles was analyzed. For example, in Ref. [28], the internal structure of the flux tube, within Abelian-projected $SU(2)$ lattice gauge theory, sets the system in the borderline between type I and type II superconductors. The masses of the dual gauge and Higgs fields turned out to be quite close, again a typical property associated with a BPS point. In the case of $SU(3)$, the fitted parameters in an effective dual QCD model led to a similar limiting behavior (see Refs. [17] and [25]), while in Ref. [27] an Abelian-like type-II superconductor was favored. However, an Abelian description cannot explain $N$-ality nor related properties (for $N \geq 4$) such as the lattice $k$-string tensions [30].

In the second part of this work, we show that there exists a choice of parameters, in the $SU(N) \to Z(N)$ model we proposed in Ref. [22], where the center string field profiles for $N = 2, 3$ satisfy Nielsen-Olesen equations, thus conciliating Abelian-like behavior with $N$-ality. Furthermore, in the $SU(2)$ case, a BPS bound is obtained, showing the fundamental BPS vortex is a minimum with respect to any, possibly non-Abelian, field deformation. This special point will certainly serve as a place to start exploring the model parameter space and verify its suitableness to accommodate

the various lattice data. BPS bounds in a non-Abelian context were previously obtained in the bosonic sector of $\mathcal{N} = 2$ supersymmetric theories. The embedding of $U(1)$ vortices in a $U(N)$ gauge model with one adjoint and $N$ fundamental scalar fields was done in Ref. [31]. With regard to center strings, previous attempts to derive relativistic BPS equations required an appropriate limit in the parameters, in order to be compatible with the original theory [32].

## II. PHYSICAL MOTIVATION FOR CENTER STRINGS

Assuming that the confining states of pure YM can be described by an effective field model, we review here why considering an $SU(N) \to Z(N)$ SSB pattern is attractive, as well as some natural phenomenological choices.

### A. A view from magnetic ensembles

Confinement scenarios based on magnetic ensembles in $SU(N)$ pure YM theory have been analyzed on the lattice (for a detailed discussion, see [33,34] and references therein). Center vortices are essentially obtained by decomposing the link variables as $U_\mu(x) = \mathcal{P}_\mu(x)Z_\mu(x)$, where $Z_\mu(x)I$ is the center element of $SU(N)$ closest to $U_\mu(x)$, and then discarding the perturbative part $\mathcal{P}_\mu(x)$. The configurations thus obtained correspond to center vortex defects located at plaquettes where $\prod Z_\mu(x) \neq 1$. In the continuum, center vortex configurations for the gluon gauge field $A_\mu$ have been parametrized in Ref. [10]. This parametrization can be rewritten in terms of a local frame in color space ($u_A$) that contains defects (see Ref. [22]),

$$A_\mu = (\mathcal{P}_\mu^A - Z_\mu^A)u_A,$$
$$Z_\mu^A = -(1/g_e)f_{ABC}^e\langle u_B, \partial_i u_C\rangle,$$
$$u_A = \mathcal{S}T_A^e\mathcal{S}^{-1}, \qquad (1)$$

$\mathcal{S} \in SU_e(N)$, and $T_A^e$, $A = 1, \ldots, N^2 - 1$, are the generators of the chromoelectric group. A closed center vortex is described by $\mathcal{S} = e^{i\chi\vec{\eta}\cdot\vec{T}^e}$, where $\chi$ is a multivalued function, changing by $2\pi$ when we go around a path linking the center vortex world sheet $\Sigma$, and $\vec{\eta}$ is $2N$ times a weight $\vec{w}$ of the fundamental representation. The dot product is understood as $\vec{\eta} \cdot \vec{T}^e = \vec{\eta}|_q T_q^e$, a combination of the Cartan generators $T_q^e$, $q = 1, \ldots, N - 1$, while the weights $\vec{w}$ are $(N - 1)$-tuples of eigenvalues for a common eigenvector. With these definitions, the Wilson loop is given by

$$W_{\mathcal{C}}[A] = \mathfrak{z}(\mathcal{C})W_C[\mathcal{P}], \quad \mathfrak{z}(\mathcal{C}) = e^{-\frac{i}{2}\int d^4x g_e s_{\mu\nu}\vec{w}_e\cdot\vec{\mathcal{F}}_{\mu\nu}(Z)}, \qquad (2)$$

$$-\mathcal{F}_{\mu\nu}^q(Z) = \frac{2\pi}{g_e}\vec{\eta}|^q\oint d^2\sigma_{\mu\nu}\delta^{(4)}(x - \bar{y}(\sigma_1, \sigma_2)), \qquad (3)$$

where $d^2\sigma_{\mu\nu}$ integrates over $\Sigma$, parametrized by $\bar{y}(\sigma_1, \sigma_2)$ (see [10,35]), and $\vec{w}_e$ is any weight of the given quark representation. The source $s_{\mu\nu}$ is localized on any surface $S(\mathcal{C})$ whose border is the Wilson loop and is constructed to give the intersection number between $S(\mathcal{C})$ and the world sheet $\Sigma$. While center vortices are good at describing $N$-ality, and have a physical lattice density scaling, the Lüscher term associated with transverse fluctuations of the string has not been observed in the center-projected data. In the pure YM context, monopoles alone do not scale toward a physical density, so they should be considered together with open center vortices, forming closed chains. Indeed, these objects have also been detected and are considered very promising to explain the different properties of the confining quark potential. As a two-dimensional object is naturally associated with an effective string theory [36], modeling the center vortex component in four-dimensional (4D) ensembles is a hard task. On the other hand, monopole ensembles can be described by a field theory. How to treat both types of degrees of freedom in a unified setting is an open problem. Here, we comment on some possible choices for the effective fields that could describe the monopole component.

Different phenomenological properties and correlations will lead to a variety of effective field models exhibiting different phases [37–41]. For example, in Ref. [41], after assuming Abelian dominance (disregarding off-diagonal fluctuations in $\mathcal{P}_\mu$), a model based on a set of complex scalar fields was obtained. In this case, the following nonzero contribution to the divergence of the dual tensor in the continuum,

$$-\partial_\nu\mathcal{F}_{\mu\nu}^q(Z) = \frac{2\pi}{g_e}2N\vec{\alpha}|^q\oint_C dy_\mu\delta^{(4)}(x - y) + \cdots, \qquad (4)$$

is initially considered. Here, $C$ is the loop where a monopole is localized, and $\vec{\alpha}$ is given by the difference of the fundamental weights carried by the pair of attached vortices, which corresponds to a root of $\mathfrak{su}(N)$. If monopole correlations were turned off, the averaged Wilson loop would be

$$\langle W\rangle = \int[D\Lambda]e^{-\int d^4x\frac{\xi}{4}(\partial_\mu\vec{\Lambda}_\nu - \partial_\nu\vec{\Lambda}_\nu - \vec{J}_{\mu\nu})^2}Z_{\alpha_1}Z_{\alpha_2}\cdots, \qquad (5)$$

$$Z_\alpha = \sum_N\frac{1}{N!}\prod_{k=1}^N[Dx_k]e^{-m\sum_{k=1}^N L_k}e^{i\frac{2\pi}{g_e}\int_{C_k}dx_\mu\vec{\alpha}\cdot\vec{\Lambda}_\mu},$$

$$\vec{J}_{\mu\nu} = g_e\vec{\beta}_e s_{\mu\nu}, \qquad (6)$$

$\vec{\beta}_e = 2N\vec{w}_e$. The Abelian gauge field $\vec{\Lambda}_\mu$ is originated from the linearization of the YM action, while the labels $\alpha_1, \alpha_2, \ldots$ refer to the positive roots $\vec{\alpha}_1, \vec{\alpha}_2, \ldots$ of $\mathfrak{su}(N)$ [$N(N - 1)/2$ possibilities].

As shown in Refs. [37–40], the right hand side in Eq. (6) is a functional determinant for a vacuum to vacuum amplitude in "particle" representation. This means that $Z_\alpha$ can be cast in the form

$$Z_\alpha = \int [D\phi_\alpha][D\bar{\phi}_\alpha] e^{-\int d^4 x \bar{\phi}_\alpha [-D_\alpha^2 + m^2]\phi_\alpha},$$

$$D_\mu^\alpha = \partial_\mu - i\frac{2\pi}{g_e}\vec{\alpha}\cdot\vec{\Lambda}_\mu. \qquad (7)$$

The SSB phase, which supports Nielsen-Olesen vortices, is observed for $m^2 < 0$ after including density-density monopole interactions [41].

Now, the inclusion of non-Abelian information in the monopole ensemble naturally leads to the embedding of Eq. (5) in a non-Abelian context. This requires an $SU(N)$ gauge field $\Lambda_\mu$, with coupling constant $g = 2\pi/g_e$, and a Higgs sector containing at least $N(N-1)$ real adjoint scalars $\psi_\alpha$, $\psi_{\bar{\alpha}}$. When the fields get Abelianized by the identifications [22],

$$\Lambda_\mu = \vec{\Lambda}_\mu^q T_q, \qquad J_{\mu\nu} = \vec{J}_{\mu\nu}|^q T_q, \qquad (8a)$$

$$\frac{\psi_\alpha + i\psi_{\bar{\alpha}}}{\sqrt{2}} = \phi_\alpha E_\alpha, \qquad \frac{\psi_\alpha - i\psi_{\bar{\alpha}}}{\sqrt{2}} = \bar{\phi}_\alpha E_{-\alpha}, \qquad (8b)$$

the average (5) should be reproduced. Here, $E_\alpha$ denotes a root vector of $\mathfrak{su}(N)$ ($\vec{\alpha}$ positive),

$$[T_q, E_\alpha] = \vec{\alpha}|_q E_\alpha, \qquad q = 1, \dots, N-1. \qquad (9)$$

In Sec. V, we will see (for $N = 2, 3$) that, in the flavor symmetric model described in Sec. II A 2, this Abelianization will be dynamically driven at a special point in parameter space. Besides the fields $\psi_\alpha$, $\psi_{\bar{\alpha}}$, that model contains a set of adjoint fields with a Cartan label $\psi_q$, $q = 0, \dots, N-1$. With a total number of flavors given by $N^2 - 1$, the fields will be denoted by $\psi_A$, with the global flavor $SU(N)$ symmetry acting on index $A$. (See Sec. II A 1.) In the next section, we review the effective description of a monopole loop carrying non-Abelian (magnetic) color degrees of freedom.

### 1. Monopole ensembles with non-Abelian degrees of freedom

Among the phenomenological information to be considered in magnetic ensembles, the introduction of non-Abelian degrees of freedom is an interesting possibility. In Ref. [42], we considered an ensemble of looplike monopoles in 4D with the coupling to the diagonal gauge field in Eq. (6) replaced by

$$u_\mu(s)I^A\Lambda_\mu^A(x(s)), \qquad I^A = T_{cd}^A \bar{z}_c z_d, \qquad u_\mu = \dot{x}_\mu.$$

This coupling was introduced in Ref. [43] to describe a classical relativistic particle interacting with a non-Abelian gauge field. The $z_a$'s are complex variables that can be thought of as those labeling coherent states $|z_1, \dots, z_D\rangle$ in a linear space of general (magnetic) color states [42] ($a$ ranges from 1 to $\mathcal{D}$, the dimension of the group representation). In fact, in the context of YM monopole ensembles, using the *nonlinear* space of Gilmore-Perelemov group coherent states is more natural (see Ref. [44]). However, when the linear state calculations are projected on the sector with total occupation number one, both descriptions coincide. This is indeed the procedure followed in our previous work, which is briefly reviewed here.

The non-Abelian coupling, together with the simplest properties that characterize a loop (length and curvature), which are physically manifested through a tension $\tau$ and stiffness $1/\xi$, leads to the ensemble

$$Z = \int [D\phi][D\phi_A] e^{-W[\phi,\phi_A]} \sum_n Z_n,$$

$$Z_n = \int [Dm]_n \exp\left[-S^0 + \sum_{k=1}^n \oint_{L_k} ds \left(ig\dot{x}_\mu^{(k)} I^A \Lambda_\mu^A(x^{(k)})\right.\right.$$

$$\left.\left. - \phi(x^{(k)}) - I^A \phi_A(x^{(k)})\right)\right],$$

$$S^0 = \sum_{k=1}^n \oint_{L_k} ds \left[\tau + \frac{1}{2}(\bar{z}_c \dot{z}_c - \dot{\bar{z}}_c z_c) + \frac{1}{2\xi}\dot{u}_\mu^{(k)}\dot{u}_\mu^{(k)}\right],$$

where $n$ sums over the number of loops. $W$ encodes some correlations among them; in particular, excluded volume effects (density-density interactions) are implemented with a $\phi^2$ term. Similarly, (magnetic) color-dependent density interactions are introduced by means of a $\phi_A^2$ term in $W$. Note that $\phi$ and $\phi_A, A = 1, \dots, \mathcal{D}$, are real fields coupled with $\rho$ and $\rho_A$, respectively,

$$\rho(x) = \sum_{k=1}^n \oint_{L_k} ds_k \delta^{(4)}(x - x_k(s_k)),$$

$$\rho_A(x) = \sum_{k=1}^n \oint_{L_k} ds_k I_A(s_k)\delta^{(4)}(x - x_k(s_k)).$$

The measure $[Dm]_n$ must integrate over all possible $n$ closed monopole worldlines. This ensemble can be computed in terms of a building block $q(x, x_0, u, u_0, \bar{z}, z_0, L)$ that gives the end-to-end probability for a line of length $L$ to start at $x_0$, with tangent $u_0$ and internal variable $z_0$, and end at $x$, with $u$, $z$. The weight for an open curve has a path-integral representation that can be obtained as the continuum limit of a polymer growth process [45]. This is controlled by a Chapman-Kolmogorov recurrence relation for diffusion in $x$ and in tangent $u$ space, thus leading $q$ to satisfy a Fokker-Planck equation [42]. Upon identifying the initial and final points of the line, we get the weight for a

closed loop. As is customary for ensembles of loops, the partition function depends on the trace of the operator appearing in the diffusion equation. Besides the trace over the values of $x$ and $u$ at the identified end points, there is one over coherent states that can be rewritten as a trace over occupation number states $|n_1, \ldots, n_{\mathcal{D}}\rangle$. In what follows, we concentrate on the contribution originated from states where all but one of the entries vanish, with the nontrivial entry being $n_a = 1$, $a = 1, \ldots, \mathcal{D}$. Other sectors will produce effective fields carrying product representations of the original $\mathcal{D}$-dimensional representation. In other words, the monopole measure is taken to be

$$
[Dm]_n \equiv \frac{1}{n!} \int_0^\infty \frac{dL_1}{L_1} \frac{dL_2}{L_2} \cdots \frac{dL_n}{L_n} \int_{\mathfrak{R}^4} d^4x_1 d^4x_2 \cdots d^4x_n
$$
$$
\times \int [Dx^{(1)}(s)]_{(x_1, L_1)} \cdots [Dx^{(n)}(s)]_{(x_n, L_n)}
$$
$$
\times \int \sum_{a_1}[Dz^{(1)}(s)]_{(a_1, a_1)} \cdots \sum_{a_n, a_n}[Dz^{(n)}(s)]_{(a_n, a_n)},
$$
(10)

where $[Dx(s)]_{(x,L)}$ integrates over loops of fixed length $L$, starting and ending at $x$, while $[Dz(s)]_{(a,a)}$ is designed to compute end-to-end probabilities, starting and ending in a state where mode $a$ has occupation number one. For smooth loops,

$$
Z = \int [D\phi] e^{-W} e^{\int_0^\infty \frac{dL}{L} \int_{\mathfrak{R}^4} d^4x \sum_a Q^{aa}(x,x,L) + \ldots},
$$
$$
Q^{aa}(x, x, L) = \int d^3u Q^{aa}(x, x, u, u, L),
$$

where $Q^{ba}(x, x_0, u, u_0, L)$ is obtained by projecting $q(x, x_0, u, u_0, \bar{z}, z_0, L)$, and gives the end-to-end probability for a line of length $L$ to start at $x_0$, with tangent $u_0$ and color $a$, and end at $x$, with $u$, $b$. This weight satisfies the projected Fokker-Plank equation,

$$
[(\partial_L - (\xi/\pi)\hat{L}_u^2 + (\tau + \phi)1 + u \cdot D]Q(x, x_0, u, u_0, L) = 0,
$$
$$
Q(x, x_0, u, u_0, 0) = \delta(x - x_0)\delta(u - u_0)1,
$$

where $Q|^{cd} = Q^{cd}$, $1$ is a $\mathcal{D} \times \mathcal{D}$ identity matrix, and $D_\mu = 1\partial_\mu - ig\Lambda_\mu^A T^A$. In the semiflexible limit, we can disregard the angular momenta $l \geq 2$ in an expansion of spherical harmonics on $S^3$ (memory loss), obtaining,

$$
Z = \int [D\phi] e^{-W} (\text{Det}O)^{-1},
$$
$$
O = -\frac{\pi}{12\xi} D_\mu D_\mu + (\phi + \tau)1 + T^A \phi_A.
$$
(11)

For an ensemble of loops carrying adjoint charges in $SU(N)$ ($\mathcal{D} = N^2 - 1$), the matrix elements of $T^A$ are proportional to the $\mathfrak{su}(N)$ structure constants. In this case, $(\text{Det}O)^{-1}$ can be represented as a path-integral over complex fields $\zeta^A$, with action density $\bar{\zeta}_A O|_{AB}\zeta_B$. The integrations over $\phi$, $\phi_A$ can easily be done as they involve a Gaussian weight $W$ and linear terms $\phi\bar{\zeta}_A\zeta_A$, $\phi_A\bar{\zeta}_B T^A|_{BC}\zeta_C$. For example, the second term is $\propto \phi_A f_{ABC}\psi_1^B \psi_2^C$, where $f_{ABC}$ are structure constants of $\mathfrak{su}(N)$ and $\psi_1^A$ ($\psi_2^A$) is the real (imaginary) part of $\zeta^A$. Then, the integration over $\phi_A$ originates a term $\langle\psi_1 \wedge \psi_2, \psi_1 \wedge \psi_2\rangle$ in the effective action. Here, we grouped the color components to form real adjoint fields $\psi_1, \psi_2 \in \mathfrak{su}(N)$.[1] Proceeding similarly with the other terms, we obtained

$$
Z = \int [D\psi] e^{-\int d^4x \mathcal{L}(\psi, \Lambda)},
$$
$$
\mathcal{L}(\psi, \Lambda) = \frac{1}{2}\langle D_\mu \psi_I, D^\mu \psi_I\rangle + \frac{\mu^2}{2}\langle\psi_I, \psi_I\rangle
$$
$$
+ \frac{\lambda}{4}\langle\psi_I \wedge \psi_J, \psi_I \wedge \psi_J\rangle + \frac{\eta}{4}\langle\psi_I, \psi_I\rangle\langle\psi_J, \psi_J\rangle,
$$

where $\psi_I$, $I = 1, 2$, $D_\mu$ acts as shown in Eq. (12), and $\mu^2 \propto \tau\xi$. These are precisely typical terms involving a pair of flavors $\alpha, \bar{\alpha}$ in the effective Yang-Mills-Higgs (YMH) model that we review below.

### 2. The Yang-Mills-Higgs model

To drive $SU(N) \to Z(N)$ SSB, at least $N$ adjoint Higgs fields $\psi_I$, $I = 1, \ldots, d$, $d \geq N$, are required [46–49]. A natural class is given by (see Ref. [22]),

$$
\mathcal{L} = \frac{\zeta}{4}\langle F_{\mu\nu}, F^{\mu\nu}\rangle + \frac{1}{2}\langle D_\mu \psi_I, D^\mu \psi_I\rangle - V_{\text{Higgs}}(\psi_I),
$$
$$
D_\mu = \partial_\mu + g\Lambda_\mu \wedge,
$$
$$
F_{\mu\nu} = \partial_\mu \Lambda_\nu - \partial_\nu \Lambda_\mu + g\Lambda_\mu \wedge \Lambda_\nu,
$$
(12)

where $\Lambda_\mu$ is a (dual) gauge field, and $I$ is a flavor index. The Higgs potential is constructed with the natural $SU(N)$ invariant terms, up to quartic order,

$$
\langle\psi_I, \psi_J\rangle, \qquad \langle\psi_I, \psi_J \wedge \psi_K\rangle,
$$
$$
\langle\psi_I \wedge \psi_J, \psi_K \wedge \psi_L\rangle, \qquad \langle\psi_I, \psi_J\rangle\langle\psi_K, \psi_L\rangle.
$$

The construction of a flavor symmetric model can be motivated in analogy with that followed for a single $SU(2)$ adjoint Higgs field $\psi$ undergoing $SU(2) \to U(1)$ SSB. This pattern is obtained from a Higgs potential whose vacua are points on $S^2$,

---

[1]We are also using the Lie algebra product $X \wedge Y = -i[X, Y]$, and the internal product $\langle X, Y\rangle = Tr(Ad(X)^\dagger Ad(Y))$, with $Ad(\cdot)$ a linear map into the adjoint representation.

$$\langle \psi, \psi \rangle - v^2 = 0.$$

A natural Higgs potential, with up to quartic terms, is then obtained by squaring the vacuum condition,

$$V_{\text{Higgs}} = \frac{\lambda}{4} (\langle \psi, \psi \rangle - v^2)^2.$$

Now, to get a flavor symmetric model with $SU(N) \to Z(N)$ SSB, we take $d = N^2 - 1$, so that the range of the flavor index coincides with that of color. Replacing $I \to A = 1, \ldots, N^2 - 1$, we denote the Higgs fields as $\psi_A$ and initially propose a Higgs potential whose vacua satisfy

$$\psi_A \wedge \psi_B - v f_{ABC} \psi_C = 0.$$

The vacua are given by a trivial point $\psi_A = 0$ plus a manifold of nontrivial vacua, where $\psi_A$ form a Lie basis. Of course, the space of vacua is invariant under the adjoint action of $SU(N)$ gauge transformations. In addition, a given Lie basis is invariant under this action iff $U \in Z(N)$. Then, a natural potential would be obtained by squaring the condition above. Using the notation $\langle X \rangle^2 = \langle X, X \rangle$,

$$V_{\text{Higgs}} = \frac{\lambda}{4} \langle \psi_A \wedge \psi_B - f_{ABC} v \psi_C \rangle^2. \qquad (13)$$

However, for this potential the trivial and nontrivial vacua are degenerate. This can be lifted by initially expanding the squares and then introducing general couplings for the quadratic, cubic, and quartic terms,[2]

$$V_{\text{Higgs}} = c + \mu^2 I_2 + \kappa I_3 + \lambda I_4, \qquad I_2 = \frac{1}{2} \langle \psi_A \rangle^2,$$

$$I_3 = \frac{1}{3} f_{ABC} \langle \psi_A, \psi_B \wedge \psi_C \rangle, \quad I_4 = \frac{1}{4} \langle \psi_A \wedge \psi_B \rangle^2. \qquad (14)$$

Besides being gauge invariant, this potential is flavor symmetric under $Ad(SU(N))$ transformations, $\psi_A \to R_{AB} \psi_B$. The constant $c$ is chosen in order for $V_{\text{Higgs}}$ to be zero when the Higgs fields assume their asymptotic vacuum values. In this manner, the asymptotic energy density of the vortex will tend to zero, and the total energy will be finite. At $\mu^2 = \frac{2}{9} \frac{\kappa^2}{\lambda}$ the degenerate case is reobtained, while for $\mu^2 < \frac{2}{9} \frac{\kappa^2}{\lambda}$ the absolute minima are given only by nontrivial vacua. For $\kappa < 0$, they are

$$\phi_A = v S T_A S^{-1}, \qquad v = -\frac{\kappa}{2\lambda} \pm \sqrt{\left(\frac{\kappa}{2\lambda}\right)^2 - \frac{\mu^2}{\lambda}},$$

which verify

---

[2]The terms $\langle \psi_A, \psi_B \rangle \langle \psi_A, \psi_B \rangle$ and $\langle \psi_A, \psi_A \rangle \langle \psi_B, \psi_B \rangle$ could also be added, although the subsequent analysis will not be essentially modified.

$$\mu^2 v + \kappa v^2 + \lambda v^3 = 0. \qquad (15)$$

According to Sec. II A, it is natural to introduce the quark sources in the form

$$S = \int d^4 x \left( \frac{\zeta}{4} \langle F_{\mu\nu} - J_{\mu\nu}, F_{\mu\nu} - J_{\mu\nu} \rangle + \frac{1}{2} \langle D_\mu \psi_A, D_\mu \psi_A \rangle \right.$$
$$\left. + V_{\text{Higgs}}(\psi_A) \right), \qquad (16)$$

where, for a given quark representation, $J_{\mu\nu}$ is given by Eqs. (6) and (8a). The quark pair, with charges $\vec{\beta}_e$ and $-\vec{\beta}_e$, will be placed on the $x^1$ axis, at $x^1 = -L/2$ and $x^1 = +L/2$, with the associated Dirac strings $J_{ij}$ running between the monopole locations and infinity.

### B. A view from phenomenology

In Sec. II A, we discussed how models with adjoint Higgs fields effectively describe ensembles of loops with adjoint charges. These are in turn the type of loops that interpolate center vortices in YM ensembles. The Abelian-like models in Ref. [41] suggest that, to describe the monopole correlations, a pair of real adjoint scalars should be included for every positive root. We also anticipated that additional flavors, for every Cartan index, will be needed to (dynamically) make contact with the Abelian-like models. Here, we review the discussion in Ref. [22] about how this class of models, when realized in an $SU(N) \to Z(N)$ SSB phase, can accommodate important lattice information regarding the confining gluon states in pure YM.

Initially, we note that in this phase the manifold of vacua is $\mathcal{M} = SU(N)/Z(N) = Ad(SU(N))$, that is, it points in the adjoint representation of $SU(N)$. As a consequence, (dual) topological degrees, with a mathematical description similar to center vortices and monopoles in pure YM, but with a completely different physical interpretation, will enter the scene. Similar to Eq. (1), they can be described by a local frame $n_A$ as follows [50]:

$$\Lambda_\mu = (\mathcal{A}_\mu^A - C_\mu^A) u_A,$$
$$C_\mu^A = -(1/g) f_{ABC} \langle n_B, \partial_i n_C \rangle,$$
$$n_A = S T_A S^{-1}, \qquad (17)$$

$$F_{ij} = (F_{ij}^A(\mathcal{A}) - F_{ij}^A(C)) n_A,$$
$$F_{ij}^A(C) = (i/g) \text{tr}(M^A R^{-1} [\partial_i, \partial_j] R), \qquad (18)$$

where $F_{ij}^A(\cdot)$ denotes the components of the non-Abelian field strength, and $R = Ad(S)$ is the adjoint representation of the map $S \in SU(N)$. In particular, $F_{ij}^A(C)$ is concentrated at the frame defects. Locally, in the asymptotic region where $\mathcal{A}_\mu^A \to 0$, $\Lambda_\mu$ is a pure gauge that is globally nontrivial when $n_A$ contains defects.

### 1. Confining fundamental center strings

Because of $\Pi_1(Ad(SU(N))) = Z(N)$, the model supports smooth (dual) center vortex solutions, or center strings. A detailed analysis of the relation between center string charges and magnetic weights, for different groups and representations, was carried out in Ref. [21]. $Z(N)$ center strings can be labeled by the weights of the different group representations,

$$S = e^{i\varphi\vec{\beta}\cdot\vec{T}}, \qquad \vec{\beta} = 2N\vec{w}. \tag{19}$$

A weight $\vec{w}$ is defined by the eigenvalues of diagonal generators corresponding to one common eigenvector,

$$[T_q, T_p] = 0, \qquad T_q\text{eigenvector} = \vec{w}|_q\text{eigenvector}.$$

When external quark sources in a given quark representation are introduced by means of the $J_{\mu\nu}$-coupling in Eqs. (16), (8a), and (6), a minimum energy configuration will be induced between them. For fundamental quarks, $\vec{\beta}_e$ is $2N$ times a fundamental weight, and a finite string characterized by a phase $S$ in Eq. (19), and one of the $N$ possible fundamental colors $\vec{\beta}_i$ (which satisfy $\vec{\beta}_1 + \cdots + \vec{\beta}_N = \vec{0}$), will be induced (see Sec. III). These weights are associated with the simplest center strings, as $e^{i2\pi\vec{\beta}_i\cdot\vec{T}} = e^{i2\pi/N}I$ is the $Z(N)$ generator.

For example, in $SU(3)$, for three external fundamental quark sources, the induced phase for the dynamical fields that form a baryon in a $Y$-junction configuration is

$$S = e^{i\chi_1\vec{\beta}_1\cdot\vec{T}}e^{i\chi_2\vec{\beta}_2\cdot\vec{T}}, \tag{20}$$

where $\chi_1$ and $\chi_2$ are multivalued when we go around a pair of curves $\mathcal{C}_1$ and $\mathcal{C}_2$. These curves coincide on a branch, so that if a center string with charge $\vec{\beta}_1$ (respectively $\vec{\beta}_2$) is leaving a pair of external monopoles (representing the green and red quarks, respectively), then a flux $\vec{\beta}_1 + \vec{\beta}_2$ will enter the third monopole, whose charge is therefore given by $-\vec{\beta}_1 - \vec{\beta}_2 = \vec{\beta}_3$, thus representing the blue quark. Note in passing that the interaction between a pair of strings with fundamental weights $\vec{\beta}_1, \vec{\beta}_2$ is expected to be attractive, as when they exactly overlap they could form an antifundamental string, lowering the energy. The analysis when strings are at a finite distance would require a non-Abelian ansatz.

### 2. Hybrid mesons

In addition to normal mesons and baryons, lattice calculations predict a rich spectrum of exotic objects. Some of them correspond to $qg\bar{q}'$ hybrid mesons where a nonsinglet color pair and a valence gluon form a colorless state. For a review, see Ref. [51]. A collaboration based at the Jefferson Lab (GlueX) is aimed at mapping gluonic excitations by searching hybrid states generated by photoproduction. In a world of heavy quarks, a successful effective model should accommodate these hybrid excitations, and, besides the normal $q\bar{q}$ potential, it should also reproduce the lattice hybrid potentials [52]. Now, if normal strings are to be seen as fundamental center strings, valence gluons should be (dual) monopolelike objects, with adjoint charges, interpolating them (color adaptors). Indeed, as explained in Ref. [22] (see also [20] and [53]), there is an exact homotopy sequence that gives support to solutions formed by different center strings interpolated by a non-Abelian monopole. The mapping required to describe this situation is

$$S = e^{i\varphi\vec{\beta}_1\cdot\vec{T}}W(x), \qquad W(x) = e^{i\theta\sqrt{N}T_\alpha}.$$

Around the North Pole,

$$S(x) \sim e^{i\varphi\vec{\beta}_1\cdot\vec{T}}.$$

Close to the South Pole, $W(x) \sim W_\alpha = e^{i\pi\sqrt{N}T_\alpha}$ becomes a Weyl reflection, so for $\vec{\alpha} = \vec{w}_1 - \vec{w}_2$ we get the behavior,

$$S(x) \sim W_\alpha e^{i\varphi\vec{\beta}_2\cdot\vec{T}},$$

and the charge of the interpolating monopole is

$$\vec{Q}_m = \frac{2\pi}{g}(\vec{\beta}_1 - \vec{\beta}_2) = \frac{2\pi}{g}2N\vec{\alpha}.$$

As the roots are the weights of the adjoint representation, which acts via commutators [cf. Eq. (9)], this monopole is naturally identified with a valence gluon with adjoint color $\vec{\alpha}$ (see also Ref. [19]). A pair of external fundamental quarks in a nonsinglet color state will induce a finite hybrid solution.

### 3. Confinement of (valence) gluons

The confinement of a valence gluon (adjoint dual monopole) is not only due to the fact that it is part of finite energy solutions that form confined quark/gluon/antiquark states. In fact, the second homotopy group of a compact group is trivial, thus implying $\Pi_2(\mathcal{M}) = \Pi_2(Ad(SU(N))) = 0$. As a consequence, our model does not have finite energy solutions for the isolated smooth adjoint monopole. This is interpreted as the absence of gluons in asymptotic states.

### 4. Lüscher terms and non-Abelian strings

Non-Abelian strings in $U(N)_{\text{gauge}} \times SU(N)_{\text{flavor}}$ models with $N$ flavors of colored fundamental scalars, undergoing SSB to a flavor-locking phase with global $SU(N)_{\text{C+F}}$, have been introduced in Refs. [19,54,55]. They possess attractive

features such as decay rates of quasistable $k$ strings [56] similar to those present in large $N$ pure YM. Non-Abelian vortices have a nontrivial moduli space where an energy scale is generated due to quantum effects. For $N \to \infty$, the internal orientational degrees in large enough strings are frozen out, and the Lüscher coefficient approaches the standard value due to transverse fluctuations. For smaller strings there is a window where light orientational modes modify this coefficient [57]. However, at finite $N$, these massless states are not expected [58], suggesting that non-Abelian strings can be compatible with the Lüscher term observed in $SU(3)$ lattice YM, which is only due to transverse fluctuations [2]. This behavior was also confirmed in $SU(2)$, with very good accuracy [59], and up to $N = 6$ for the fundamental string ground state [60].

Our model in Eq. (14) is based on $N^2 - 1$ flavors of colored adjoint scalars and has an $SU(N)_{\text{gauge}} \times SU(N)_{\text{flavor}}$ symmetry, realized in the adjoint representation. In the SSB phase the vacuum displays a global $Z(N) \times Ad(SU(N))_{\text{C+F}}$ symmetry. Then, properties similar to those previously discussed are expected; a careful analysis of these aspects will be deferred to a future work. Here, we would like to emphasize that, in view of II A, a model based on adjoint rather than fundamental Higgs fields is a natural choice. We also note that the flavor symmetry is introduced as it restricts the possible terms in the potential, and it simplifies the mathematical structure, the reduction to Abelian-like equations, as well as the search for a BPS point. However, at this stage, we have no additional motivation for this symmetry, so we should be open to also consider nonflavor symmetric models with fewer adjoint Higgs fields and the same SSB pattern. Before proceeding, in order to avoid confusion between the various objects discussed in the effective model, it is convenient to give a brief list of them:

*dual fields*, effective fields aimed at describing magnetic YM ensembles;

*center string*, confining YM string represented in dual language;

*quarks*, fundamental monopole sources at string ends (external);

*adjoint quarks*, adjoint monopole sources (external);

*valence gluons*, dynamical adjoint monopoles (internal). They interpolate center strings with different weights.

## III. THE CENTER STRING BETWEEN A QUARK-ANTIQUARK PAIR

In the presence of sources, the energy functional is [cf. Eq. (16)],[3]

$$E = \int d^3 x (\rho_B + \rho_K + V_{\text{Higgs}}),    (21)$$

$$\rho_B = \frac{1}{4} \langle F_{ij} - J_{ij} \rangle^2, \qquad \rho_K = \frac{1}{2} \langle D_i \psi_A \rangle^2.    (22)$$

This is minimized by the static equations,

$$D_j(F_{ij} - J_{ij}) = ig[\psi_A, D_i \psi_A],    (23a)$$

$$D_i D_i \psi_A = \mu^2 \psi_A + \kappa f_{ABC} \psi_B \wedge \psi_C + \lambda \psi_B \wedge (\psi_A \wedge \psi_B).    (23b)$$

Let us consider a center string, ending at external monopolelike sources, with fundamental weight $\vec{\beta}$. Because of cylindrical symmetry, all field profile functions in our ansatz are required to be $\varphi$ independent. Taking in Eq. (17),

$$S = e^{i\varphi \vec{\beta} \cdot \vec{T}},    (24)$$

$\mathcal{A}_\mu^q = \frac{(a-1)}{g} \partial_i \varphi \vec{\beta}|_q$, and the other components as zero, the gauge field ansatz is

$$\Lambda_i = \frac{1}{g} a \partial_i \varphi \vec{\beta} \cdot \vec{T}.    (25)$$

For $SU(2)$ and $SU(3)$, the magnetic weights are one- and two-component tuples; they can be chosen as $\vec{\beta} = \sqrt{2}$ and $\vec{\beta} = (\sqrt{3}/2, 1)$, respectively. Besides the Cartan generators, the Lie algebra basis is completed with the off-diagonal generators $T_\alpha = (E_\alpha + E_{-\alpha})/\sqrt{2}$, $T_{\bar{\alpha}} = -i(E_\alpha - E_{-\alpha})/\sqrt{2}$, where $E_{\pm\alpha}$ are the root vectors associated with the positive and negative roots $\pm \vec{\alpha}$, respectively. For the Higgs field ansatz, using that $S T_q S^{-1} = T_q$, and

$$S T_\alpha S^{-1} = \cos(\vec{\alpha} \cdot \vec{\beta}) \varphi T_\alpha - \sin(\vec{\alpha} \cdot \vec{\beta}) \varphi T_{\bar{\alpha}},$$
$$S T_{\bar{\alpha}} S^{-1} = \sin(\vec{\alpha} \cdot \vec{\beta}) \varphi T_\alpha + \cos(\vec{\alpha} \cdot \vec{\beta}) \varphi T_{\bar{\alpha}},    (26)$$

we propose the form

(i) $SU(2)$:

$$\psi_1 = h_1 T_1, \quad \psi_{\alpha_1} = h S T_{\alpha_1} S^{-1}, \quad \psi_{\bar{\alpha}_1} = h S T_{\bar{\alpha}_1} S^{-1};    (27)$$

(ii) $SU(3)$:

$$\psi_q = h_{qp} T_p, \quad h_{qp} = \frac{1}{4} h_1 \vec{\beta}|_q \vec{\beta}|_p + 3 h_2 \vec{\alpha}_2|_q \vec{\alpha}_2|_p,    (28)$$

---

[3]By a redefinition of the coupling constant $g$, the $\zeta$ factor can be set to 1.

$$\psi_{\alpha_1} = hST_{\alpha_1}S^{-1}, \quad \psi_{\alpha_2} = h_0 T_{\alpha_2}, \quad \psi_{\alpha_3} = hST_{\alpha_3}S^{-1},$$
(29)

$$\psi_{\tilde{\alpha}_1} = hST_{\tilde{\alpha}_1}S^{-1}, \quad \psi_{\tilde{\alpha}_2} = h_0 T_{\tilde{\alpha}_2}, \quad \psi_{\tilde{\alpha}_3} = hST_{\tilde{\alpha}_3}S^{-1}.$$
(30)

Note that for $SU(2)$ there is a single positive root $\alpha_1 = 1/\sqrt{2}$, so that the pair $\psi_{\alpha_1}$, $\psi_{\tilde{\alpha}_1}$ rotates once when we go around the center string. On the other hand, in $SU(3)$, the three positive roots satisfy $\vec{\alpha}_1 \cdot \vec{\beta} = 1$, $\vec{\alpha}_2 \cdot \vec{\beta} = 0$, $\vec{\alpha}_3 \cdot \vec{\beta} = 1$. Then, in this case there is a pair $\psi_{\alpha_2}$, $\psi_{\tilde{\alpha}_2}$ that does not rotate, while the others rotate once. In both cases, finite energy solutions require the asymptotic boundary conditions,

$$a \to 1, \quad h \to v, \quad h_1 \to v$$
(31)

[in $SU(3)$, we also have $h_0 \to v$, $h_2 \to v$]. There are also regularity conditions to be satisfied. The field strength tensor is

$$F_{ij} = \frac{1}{g}\{(\partial_i a \partial_j \varphi - \partial_j a \partial_i \varphi) + a[\partial_i, \partial_j]\varphi\}\vec{\beta} \cdot \vec{T}, \quad (32)$$

where $[\partial_2, \partial_3]\varphi = 2\pi\delta^{(2)}(x^2, x^3)$. Then, when approaching the $x^1$ axis, we require

$$a \to 0, \quad h \to 0, \quad \text{when } |x^1| < L/2, \quad (33)$$

$$a \to 1, \quad h \to v, \quad \text{when } |x^1| > L/2. \quad (34)$$

In this manner, the delta singularity in Eq. (32), present for $|x^1| > L/2$, is canceled against the Dirac string $J_{ij}$, leaving an energy density contribution $(1/4)(F_{ij} - J_{ij})^2$ that is smooth everywhere. On the other hand, the profile functions $h_0$, $h_1$, and $h_2$, associated with Higgs fields that do not rotate, are finite on the $x^1$ axis. They are not required to vanish there.

Now, let us consider curvilinear coordinates $\xi^1$, $\xi^2$, $\xi^3$ in $R^3$, $x = x(\xi)$. To represent vectors $A = A^i\mathbf{e}_i = A_i\mathbf{e}^i$, we can use either covariant or contravariant basis vectors $\mathbf{e}_i$ or $\mathbf{e}^i$, with Cartesian components, $\mathbf{e}_i|_{x^j} = \frac{\partial x^j}{\partial \xi^i}$, $\mathbf{e}^i|_{x^j} = \frac{\partial \xi^i}{\partial x^j}$. The metric for contravariant and covariant coordinates satisfy $g_{ij}g^{jk} = \delta_i^k$,

$$dx_k dx_k = g_{ij}d\xi^i d\xi^j, \quad \frac{\partial \psi}{\partial x^k}\frac{\partial \psi}{\partial x^k} = g^{ij}\frac{\partial \psi}{\partial \xi^i}\frac{\partial \psi}{\partial \xi^j}.$$

In curvilinear coordinates, the total energy is[4]

$$E = \int d^3\xi\sqrt{g}\left(\frac{1}{4}\langle F_{ij}, F^{ij}\rangle + \frac{1}{2}\langle D_i\psi_A, D^i\psi_A\rangle + V_{\text{Higgs}}\right)$$

$$= \int d^3\xi\sqrt{g}\left(\frac{1}{4}g^{ik}g^{jl}\langle F_{ij}, F_{kl}\rangle\right.$$

$$\left. + \frac{1}{2}g^{ij}\langle D_i\psi_A, D_j\psi_A\rangle + V_{\text{Higgs}}\right),$$

while the components of the chromomagnetic field $B = B_i\mathbf{e}^i$ are

$$B_i = \frac{1}{2}g_{ij}[\det g^{rs}]^{\frac{1}{2}}\epsilon_{jkl}F_{kl},$$

$$F_{kl} = \left(\frac{\partial A_l}{\partial \xi^k} - \frac{\partial A_k}{\partial \xi^l} + gA_k\wedge A_l\right). \quad (35)$$

Let us consider any system of orthogonal coordinates, where $\xi^3$ is the polar angle with respect to the $x^1$ axis, $\xi^3 = \varphi \in [0, 2\pi)$. That is, the gauge field ansatz (25) is

$$A = \frac{1}{g}a\mathbf{e}^3\vec{\beta} \cdot \vec{T}, \quad a = a(\xi^1, \xi^2), \quad (36)$$

and the gauge field covariant components are

$$A_1 = 0, \quad A_2 = 0, \quad A_3 = \frac{a}{g}\vec{\beta} \cdot \vec{T}. \quad (37)$$

Using the scale factors $s_i = |\mathbf{e}_i|$ and the properties

$$|\mathbf{e}^i| = s_i^{-1}, \quad g_{ii} = s_i^2, \quad g^{ii} = s_i^{-2}, \quad \sqrt{g} = s_1 s_2 s_3, \quad (38)$$

we obtain

$$B_1 = \frac{s_1}{gs_2 s_3}\partial_2 a\vec{\beta} \cdot \vec{T}, \quad B_2 = -\frac{s_2}{gs_1 s_3}\partial_1 a\vec{\beta} \cdot \vec{T}, \quad B_3 = 0,$$
(39)

$$\rho_B = \frac{(N-1)}{g^2(s_3)^2}[(s_2)^{-2}(\partial_2 a)^2 + (s_1)^{-2}(\partial_1 a)^2]. \quad (40)$$

In addition, the covariant components of the curl of $B$ are $\nabla \times B|_1 = \nabla \times B|_2 = 0$,

$$\nabla \times B|_3 = -\frac{s_3}{gs_1 s_2}\left(\partial_1\left(\frac{s_2}{s_1 s_3}\partial_1 a\right) + \partial_2\left(\frac{s_1}{s_2 s_3}\partial_2 a\right)\right)\vec{\beta} \cdot \vec{T}. \quad (41)$$

---

[4]In these equations, the indices $i, j, ...,$ refer to curvilinear coordinates.

Using our ansatz, it is easy to see that the right-hand side of Eq. (23a) is also along the $\mathbf{e}^3$ direction and that after putting $h_\alpha = h_{\bar\alpha}$ the Lie algebra directions on the left- and right-hand sides of the equations also coincide. In both cases, $N = 2, 3$, we get

$$-\frac{s_3}{gs_1 s_2}\left(\partial_1\left(\frac{s_2}{s_1 s_3}\partial_1 a\right) + \partial_2\left(\frac{s_1}{s_2 s_3}\partial_2 a\right)\right) = g(1-a)h^2.$$
(42)

As $h_\alpha = h_{\bar\alpha}$, after working out the algebra, the field equations for $\psi_\alpha$ and $\psi_{\bar\alpha}$ give the same information. They can be simplified using

$$\nabla \cdot A \propto \partial^2 \varphi = 0, \qquad \nabla h(\xi^1, \xi^2) \cdot \nabla \varphi = 0.$$

In what follows, we detail the remaining equations and information related with the kinetic and potential energy densities for the Higgs fields. Defining

$$\hat{O}h = \partial^2 h - \frac{(1-a)^2}{(s_3)^2}h,$$

$$\partial^2 f = \frac{1}{s_1 s_2 s_3}\left[\frac{\partial}{\partial\xi^1}\left(\frac{s_2 s_3}{s_1}\frac{\partial f}{\partial\xi^1}\right) + \frac{\partial}{\partial\xi^2}\left(\frac{s_3 s_1}{s_2}\frac{\partial f}{\partial\xi^2}\right)\right],$$

$SU(2)$:

$$\hat{O}h = \mu^2 h + \kappa h h_1 + (\lambda/2)h(h^2 + h_1^2),$$
(43)

$$\partial^2 h_1 = \mu^2 h_1 + (\kappa + \lambda h_1)h^2,$$
(44)

$$\rho_K = [(s_1^{-1}\partial_1 h)^2 + (s_2^{-1}\partial_2 h)^2] + (s_3^{-1}h(a-1))^2$$
$$+ \frac{1}{2}[(s_1^{-1}\partial_1 h_1)^2 + (s_2^{-1}\partial_2 h_1)^2],$$
(45)

$$I_2 = h_1^2/2 + h^2, \quad I_3 = h_1 h^2, \quad I_4 = h_1^2 h^2/2 + h^4/4,$$
(46)

$$c = -[(3/2)\mu^2 v^2 + \kappa v^3 + (3/4)\lambda v^4].$$
(47)

$SU(3)$:

$$\hat{O}h = \mu^2 h + (\kappa/6)h(2h_0 + 3h_1 + h_2)$$
$$+ (\lambda/12)h(6h^2 + 2h_0^2 + 3h_1^2 + h_2^2),$$
(48)

$$\partial^2 h_0 = \mu^2 h_0 + (\kappa/3)(2h_0 h_2 + h^2)$$
$$+ (\lambda/3)h_0(h_0^2 + h^2 + h_2^2),$$
(49)

$$\partial^2 h_1 = \mu^2 h_1 + \kappa h^2 + \lambda h^2 h_1,$$
(50)

$$\partial^2 h_2 = \mu^2 h_2 + (\kappa/3)(2h_0^2 + h^2) + (\lambda/3)h_2(2h_0^2 + h^2),$$
(51)

$$\rho_K = 2[(s_1^{-1}\partial_1 h)^2 + (s_2^{-1}\partial_2 h)^2 + (s_3^{-1}h(a-1))^2]$$
$$+ (s_1^{-1}\partial_1 h_0)^2 + (s_2^{-1}\partial_2 h_0)^2 + \frac{1}{2}[(s_1^{-1}\partial_1 h_1)^2$$
$$+ (s_2^{-1}\partial_2 h_1)^2 + (s_1^{-1}\partial_1 h_2)^2 + (s_2^{-1}\partial_2 h_2)^2],$$
(52)

$$I_2 = 2h^2 + h_0^2 + h_1^2/2 + h_2^2/2,$$
(53)

$$I_3 = h_1 h^2 + h_2 h^2/3 + (2/3)[h_2 h_0^2 + h_0 h^2],$$
(54)

$$I_4 = h_1^2 h^2/2 + h_2^2 h^2/6 + h_0^2(h_2^2 + h^2)/3 + h^4/2 + h_0^4/6,$$
(55)

$$c = -[4\mu^2 v^2 + (8/3)\kappa v^3 + 2\lambda v^4].$$
(56)

## IV. NUMERICAL ANALYSIS

### A. Infinite center string

Let us initially consider the simpler case of an infinite string. In this way we can gain a quick understanding of how the solutions behave under the variation of parameters, and we can also check the suitableness of the numerical methods we will use. If the quarks are infinitely far apart, the problem is invariant under translations along the $x^1$ axis. In addition, because of rotational symmetry in the $(x^2, x^3)$ plane, the problem becomes purely radial (and thus one dimensional), strongly reducing the difficulty of the numerical energy minimization. In this case, it is natural to use cylindrical coordinates,

$$\xi^1 \in (-\infty, \infty), \qquad \xi^2 = \rho \in [0, \infty), \qquad \xi^3 = \varphi \in [0, 2\pi),$$
$$x^1 = \xi^1, \qquad x^2 = \xi^2 \cos\xi^3, \qquad x^3 = \xi^2 \sin\xi^3,$$
$$s_1 = 1, \qquad s_2 = 1, \qquad s_3 = \xi^2.$$
(57)

### 1. $SU(2)$

In this section we will focus on $SU(2)$; the case of $SU(3)$ is analogous and will be shortly touched upon in Sec. IV A 2. For $SU(2)$, using Eqs. (40) and (45), the energy density per unit length takes the form

$$2\pi \int_0^\infty d\rho\rho\left(\frac{1}{g^2\rho^2}a'(\rho)^2 + h'(\rho)^2 + \frac{1}{2}h_1'(\rho)^2\right.$$
$$\left. + \frac{1}{\rho^2}h(\rho)^2(1 - a(\rho))^2 + V_{\text{Higgs}}\right).$$
(58)

To minimize this functional, we will use a Fourier finite elements method. In short, the procedure is as follows: Initially, we modify the problem until we have one on a finite interval, with simpler boundary conditions, such that all unknown functions go to zero at the boundaries. Next, we use a Fourier series to expand them. Cutting off this

series at a finite order, we plug the ansätze into the energy and minimize with respect to the Fourier coefficients.

With this in mind, let us start by looking at the boundary conditions. When $\rho \to 0$, we must have $a \to 0$, $h \to 0$, and $h_1$ regular. In this limit, assuming the leading term of $h$ is proportional to $\rho^i$, the equation for $h$ yields at lowest order in $\rho$

$$i(i-1) + i - 1 = 0 \Leftrightarrow i = \pm 1.$$

The solution $i = +1$ satisfies the boundary conditions. Proceeding similarly with the equation for $a$, one finds that the lowest order must be either $\rho^4$ (in which case the leading terms originating from $a$ will cancel the one from the $h^2$ term) or $\rho^2$ (in which case the leading terms from $a$ cancel amongst each other and are of lower order than that of $h^2$). We can simply assume that the Taylor series starts with a term in $\rho^2$, as this will cover both cases. Finally, no condition on the leading-order term of $h_1$ is obtained, but it turns out that the term linear in $\rho$ must vanish. We thus find the following small $\rho$ behaviors:

$$a(\rho) \approx a_2 \rho^2 + a_3 \rho^3 + \cdots, \tag{59a}$$

$$h(\rho) \approx b_1 \rho + b_2 \rho^2 + \cdots, \tag{59b}$$

$$h_1(\rho) \approx c_0 + c_2 \rho^2 + \cdots, \tag{59c}$$

where the dots simply continue the Taylor expansions.

When $\rho \to \infty$, we need $a \to 1$, $h \to v$, and $h_1 \to v$. As the theory is massive, due to symmetry breaking, we can expect the functions to reach their asymptotic values exponentially fast. In particular, the asymptotic behavior of $a$ is found to be

$$a(\rho) \sim 1 + \gamma e^{-gv\rho}, \tag{59}$$

with an undetermined constant $\gamma$. Therefore, let us introduce the variable $t = \tanh gv\rho$ with $t \in [0, 1]$. In this new variable, $a$ will be linear when $\rho \to \infty$ (and thus $t \to 1$). In general, the functions $h$ and $h_1$ will not have the same exponential factor at infinity, but this will not cause any problems as long as the correct asymptotic value is reached: their behavior will simply be nonlinear in $t$. It is easily seen that the small-$\rho$ behavior in (59) will still be valid with the replacement of $\rho$ by $t$. In effect, we have the series

$$t = gv\rho + \frac{(gv\rho)^3}{3} + \cdots,$$

with a vanishing second-order term, so the leading terms will remain leading, and the linear term in $h_1$ will still be absent.

Recapitulating, we can propose the ansätze

$$a(t) = t^2 + t\alpha(t), \tag{60a}$$

$$h(t) = vt + \eta(t), \tag{60b}$$

$$h_1(t) = vt^2 + \frac{h_1(0)}{2}(1 + \cos \pi t) + t\eta_1(t), \tag{60c}$$

where $\alpha(t)$, $\eta(t)$, and $\eta_1(t)$ are smooth functions in the interval $t \in [0, 1]$ that vanish both at $t = 0$ and at $t = 1$. Then, these new functions can be represented by means of a Fourier series only in terms of $\sin n\pi t$, $n \in \mathbb{N} \backslash \{0\}$. In other words, the most general profiles can be expanded as

$$a(t) = t^2 + t \sum_{n=1}^{\infty} a_n \sin n\pi t, \tag{61a}$$

$$h(t) = vt + \sum_{n=1}^{\infty} b_n \sin n\pi t, \tag{61b}$$

$$h_1(t) = vt^2 + \frac{c_0}{2}(1 + \cos \pi t) + t \sum_{n=1}^{\infty} c_n \sin n\pi t. \tag{61c}$$

Then, approximate static stable solutions are found by limiting the previous expressions to some finite order, plugging the functions into the energy density and minimizing with respect to the unknown coefficients. These steps can easily be performed using the computer algebra package *Mathematica*. We would like to emphasize that it is not necessary to transform the energy integral (58) to the new variable $t$, as we can simply plug $t = \tanh gv\rho$ into our ansätze and do the computations using $\rho$ as a variable.

Figure 1 shows the results of the numerical minimization for a certain set of parameter values. The continuous lines include six Fourier modes for each of the unknown functions. For reference, the approximation with one Fourier mode less, for each profile function, is shown in a dashed line. One can see that the approximation is already quite good and the two curves differ noticeably only in the case of $a$.

### 2. SU(3)

As mentioned before, the $SU(2)$ and $SU(3)$ cases are completely analogous. The main difference is that there are two more unknown profiles, $h_0$ and $h_2$ [cf. Eqs. (48) and (51)], and they behave exactly like $h_1$ in Eq. (59c). Figure 2 shows our results for $SU(3)$; again, convergence is quite good and only in the case of $a$ do the approximations with three or four Fourier modes noticeably differ from each other.
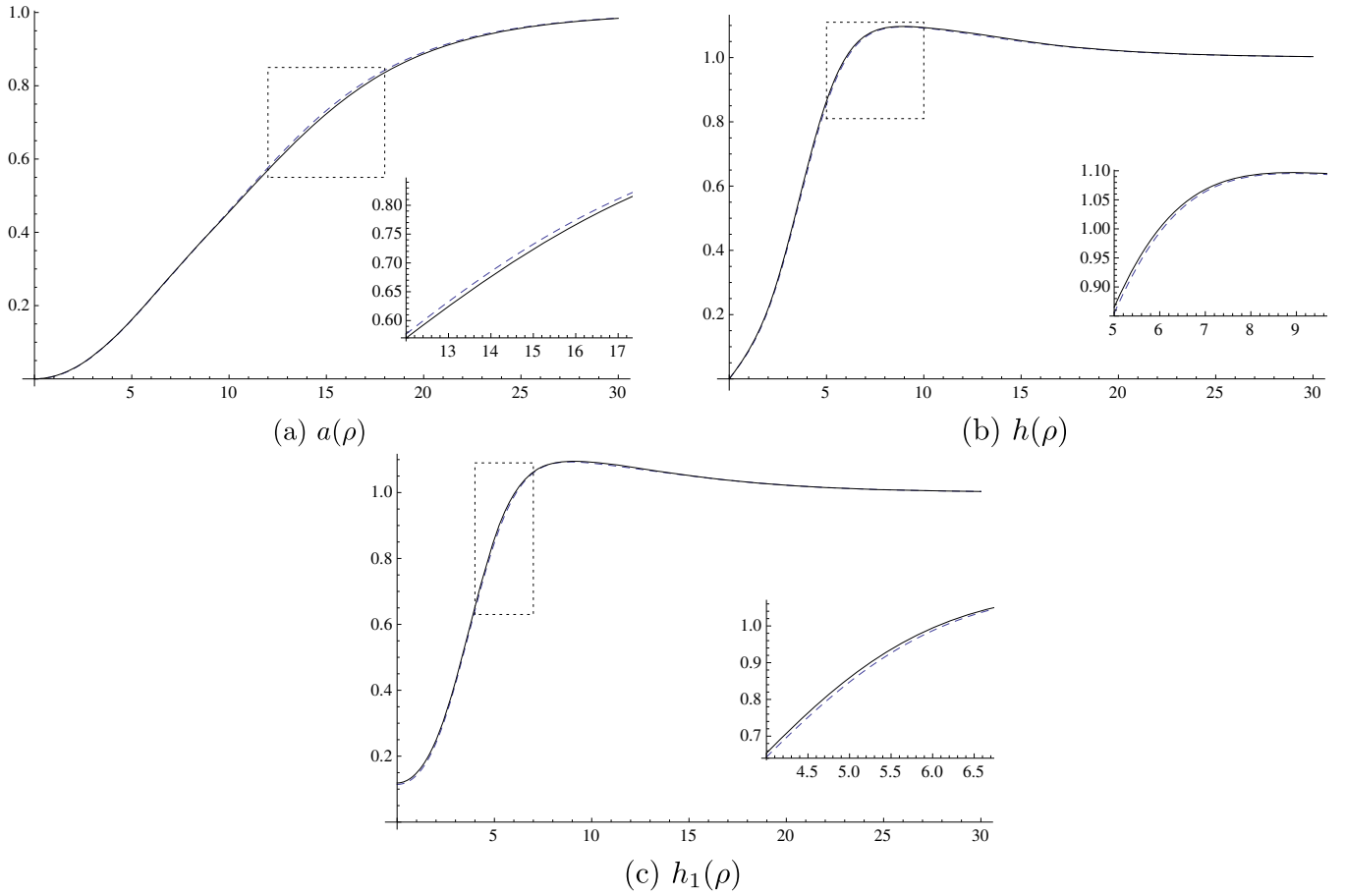
(a) $a(\rho)$



(b) $h(\rho)$



(c) $h_1(\rho)$

FIG. 1.   [$SU(2)$, $g = 0.1$, $\mu = 1$, $\kappa = -2$, $\lambda = 1$, $v = 1$.] The plots show the infinite string profiles. The dashed lines include Fourier coefficients up to the fifth order (the term with $\sin 5\pi t$), while the continuous ones include one more Fourier mode. Each of the plots is accompanied by a zoomed-in plot (which zooms in on the part marked with a box in the main plot) to see more clearly how far the two lines are from each other. One can see that the numerics have converged quite well and the two successive approximations are almost on top of each other.

## B. Finite center string

For finite strings, it is convenient to use prolate sphe-roidal coordinates with foci on the $x^1$ axis,

$$x^1 = \frac{L}{2} \cosh \xi^1 \cos \xi^2,$$

$$x^2 = \frac{L}{2} \sinh \xi^1 \sin \xi^2 \cos \xi^3,$$

$$x^3 = \frac{L}{2} \sinh \xi^1 \sin \xi^2 \sin \xi^3,$$

where $\xi^1$ is non-negative, $\xi^2 \in [0, \pi]$, $\xi^3 \in [0, 2\pi)$. The scale factors are

$$s_1 = s_2 = s = \frac{L}{2} \sqrt{\sinh^2(\xi^1) + \sin^2(\xi^2)},$$

$$s_3 = \frac{L}{2} \sinh \xi^1 \sin \xi^2. \tag{62}$$

Defining $\sigma = \sinh \xi^1 \in [0, \infty)$, together with $\xi^2 = \nu$ and $\xi^3 = \varphi$, the quark and antiquark are located at the foci described by $\sigma = 0$, $\nu = 0$ and $\sigma = 0$, $\nu = \pi$, respectively. The line joining them is given by $\sigma = 0$, $\nu \in [0, \pi]$. The semi-infinite lines extending from $x^1 = L/2$ to $+\infty$ and from $x^1 = -L/2$ to $-\infty$, on the $x^1$ axis, are given by $\sigma \in (0, \infty)$, $\nu = 0$ and $\sigma \in (0, \infty)$, $\nu = \pi$, respectively.

Then, the asymptotic boundary conditions, when $\sigma \to \infty$, are as follows:

$$a(\sigma, \nu) \to 1, \qquad h(\sigma, \nu) \to v, \qquad h_1(\sigma, \nu) \to v. \tag{63}$$

The regularity conditions, when $\sigma \to 0$, $\nu \in [0, \pi]$, are

$$a(\sigma, \nu) \to 0, \qquad h(\sigma, \nu) \to 0, \tag{64}$$

while for $\nu \to 0$ or $\nu \to \pi$, with $\sigma \in (0, \infty)$, we require

$$a(\sigma, \nu) \to 1, \qquad h(\sigma, \nu) \to v. \tag{65}$$

(a) $a(\rho)$

(b) $h(\rho)$

(c) $h_0(\rho)$

(d) $h_1(\rho)$

(e) $h_2(\rho)$
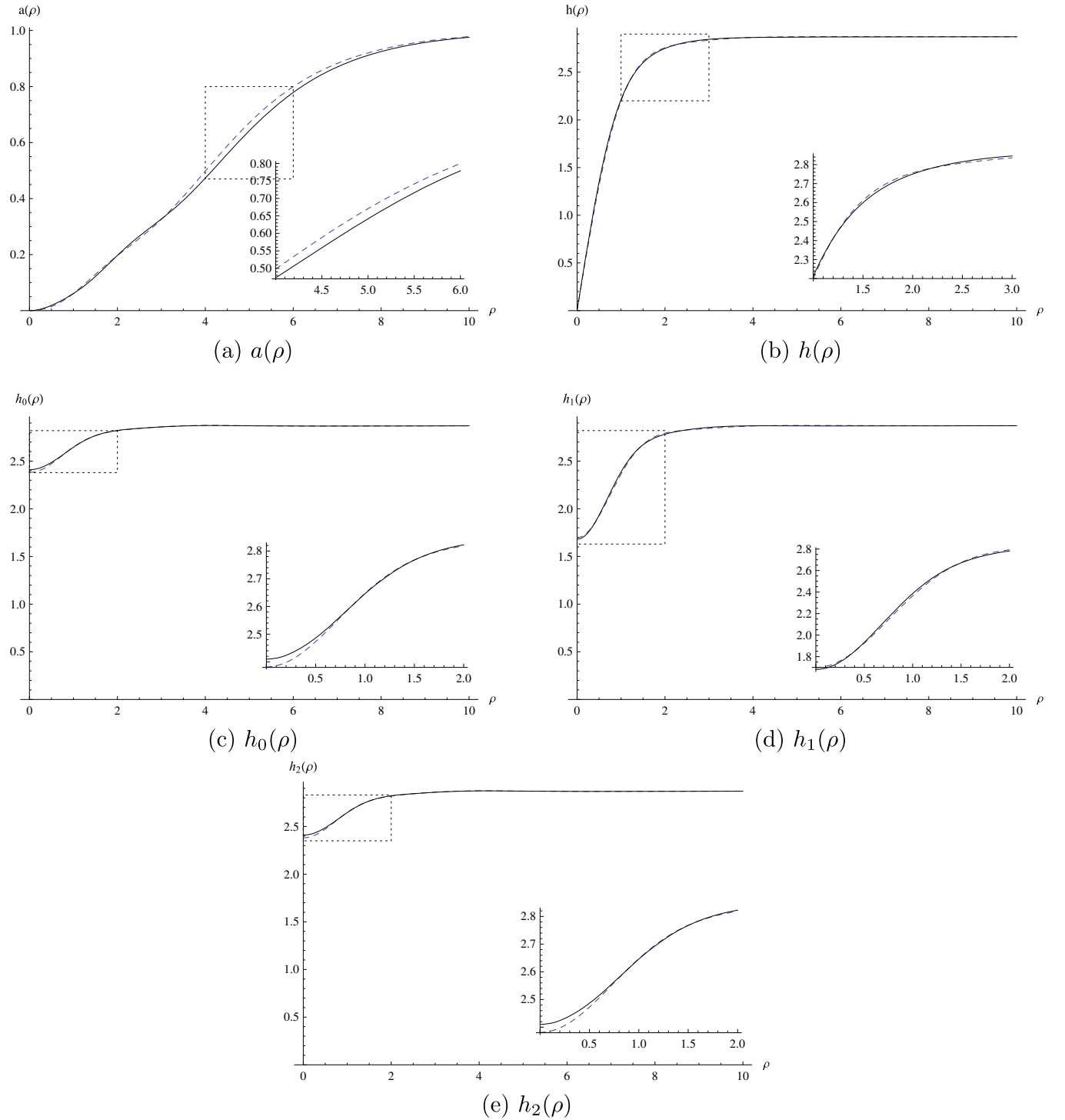
FIG. 2. $[SU(3), g = 0.1, \mu = 1.8, \kappa = -4, \lambda = 1, v = 2.87.]$ The plots show, in that order, the infinite string profiles $a$, $h$, $h_0$, $h_1$, and $h_2$, as functions of $\rho$, with accompanying zoom on the marked region. In this case the dashed lines include three Fourier modes for each of the unknown functions, while the continuous ones include four.

Finally, for $\sigma \in [0, \infty)$, $h_1$ is finite. The $SU(2)$ Eqs. (42)–(44) become

$$(1 + \sigma^2)\partial_\sigma^2 a + \partial_\nu^2 a - \left(\frac{\partial_\sigma a}{\sigma} + \frac{\partial_\nu a}{\tan \nu}\right) = \frac{L^2}{4} g^2(\sigma^2 + \sin^2 \nu) h^2(a - 1), \tag{66a}$$

$$(1 + \sigma^2)\partial_\sigma^2 h + \partial_\nu^2 h + (1 + 2\sigma^2)\frac{\partial_\sigma h}{\sigma} + \frac{\partial_\nu h}{\tan \nu}$$

$$- \frac{\sigma^2 + \sin^2 \nu}{\sigma^2 \sin^2 \nu} h(a - 1)^2 = \frac{L^2}{4}(\sigma^2 + \sin^2 \nu)(\mu^2 h + \kappa h h_1$$

$$+ (\lambda/2)h(h^2 + h_1^2)), \tag{66b}$$

$$(1 + \sigma^2)\partial_\sigma^2 h_1 + \partial_\nu^2 h_1 + (1 + 2\sigma^2)\frac{\partial_\sigma h_1}{\sigma} + \frac{\partial_\nu h_1}{\tan \nu}$$

$$= \frac{L^2}{4}(\sigma^2 + \sin^2\nu)(\mu^2 h_1 + (\kappa + \lambda h_1)h^2). \tag{66c}$$

Now, expanding around $\sigma = 0$ with $\nu$-dependent coefficients, and around $\nu = 0$ with $\sigma$-dependent coefficients, we obtain

$$a(\sigma, \nu) \approx a_2(\nu)\sigma^2 + a_3(\nu)\sigma^3 + \cdots,$$

$$a(\sigma, \nu) \approx 1 + a_2(\sigma)\nu^2 + \cdots$$

$$h(\sigma, \nu) \approx b_1(\nu)\sigma + b_2(\nu)\sigma^2 + \cdots,$$

$$h(\sigma, \nu) \approx v + b_2(\sigma)\nu^2 + \cdots$$

$$h_1(\sigma, \nu) \approx c_0(\nu) + c_2(\nu)\sigma^2 + \cdots,$$

$$h_1(\sigma, \nu) \approx c_0(\sigma) + c_2(\sigma)\nu^2 + \cdots,$$

and similar expressions around $\nu = \pi$, in powers of $(\nu - \pi)$. Around the quarks, the situation is more subtle. Setting $\sigma = r\cos\alpha$, $\nu = r\sin\alpha$ and considering series expansions around $r = 0$, with $\alpha$-dependent coefficients, we get

$$a(r, \alpha) \approx \cos^2\alpha\left[1 - r^2\sin^2\alpha\left(\frac{1}{6}\sin^2\alpha + \frac{1}{2}\cos^2\alpha\right)\right.$$

$$\left. + a_4(\alpha)r^4 + \cdots\right],$$

$$h(r, \alpha) \approx b_0(\alpha) + \cdots,$$

$$h_1(r, \alpha) \approx c_0(\alpha) + \cdots.$$

The following functions obey all these regularity and boundary conditions:

$$a(\sigma, \nu) \approx \frac{\sigma^2}{\sigma^2 + \sin^2\nu}\left(1 - \frac{1}{2}\sin^2\nu\right) + \mathcal{O}(\sigma^2\nu^2), \tag{67a}$$

$$h(\sigma, \nu) \approx \frac{v\sigma^2}{\sigma^2 + \sin^2\nu} + \mathcal{O}(\sigma\nu^2), \tag{67b}$$

$$h_1(\sigma, \nu) \approx c(\sigma, \nu), \qquad \frac{\partial c}{\partial \sigma}(0, \nu) = 0, \qquad \frac{\partial c}{\partial \nu}(\sigma, 0) = 0. \tag{67c}$$

Note that the first term in Eq. (67a) can be rewritten as

$$\frac{\sigma^2}{\sigma^2 + \sin^2\nu}\left(1 - \frac{1}{2}\sin^2\nu\right) = \frac{x^1 - L/2 + \sqrt{(x^1 - L/2)^2 + \rho^2}}{2\sqrt{(x^1 - L/2)^2 + \rho^2}}$$

$$+ \mathcal{O}((\text{distance to quark})^4)$$

for the quark at $x^1 = +L/2$, and a similar expression, with $x^1 - L/2$ replaced by $x^1 + L/2$, for the quark at $x^1 = -L/2$. The corresponding contributions to the energy are

$$2\pi\int_0^\infty d\rho \int_{-\infty}^{+\infty} dx^1 \frac{1}{4g^2}\frac{\rho}{((x^1 \mp L/2)^2 + \rho^2)^2}. \tag{68}$$

These are $L$-independent divergences, which obviously correspond to the quark self-energies. As usual, we will subtract them to get a finite total energy.

Now, we can follow a procedure similar to that used for infinite vortices. Initially, we observe that, when $\sigma \to \infty$, $a$ behaves like $\sim 1 + \gamma(\nu)e^{-Lgv\sigma/2}$. Then, introducing the variable $t = \tanh Lgv\sigma/2$, and defining

$$f(t, \nu) = \frac{t^2(1 - t^2)^{-1} - \frac{1}{3}t^4}{t^2(1 - t^2)^{-1} + (\frac{Lgv}{2})^2\sin^2\nu - \frac{1}{3}t^4},$$

$$g(t, \nu) = \left(1 - \frac{1}{2}(1 - t^2)\sin^2\nu\right),$$

we can introduce the ansätze,

$$a(t, \nu) = f(t, \nu)g(t, \nu) + t\sin\nu\alpha(t, \nu), \tag{69a}$$

$$h(t, \nu) = vf(t, \nu) + \sin\nu\eta(t, \nu) \tag{69b}$$

(note that the meaning of $t$ used here is different from that used in Sec. IV A 1). The new unknown functions $\alpha(t, \nu)$ and $\eta(t, \nu)$ are smooth in the region $(\sigma, \nu) \in [0, \infty) \times [0, \pi]$ and must vanish when $\sigma = 0$, $\sigma \to \infty$, $\nu = 0$, or $\nu = \pi$. In terms of the variables $(t, \nu)$, they vanish on the border of the square $[0, 1) \times [0, \pi]$, so they can be Fourier expanded in terms of the basis elements $\sin(n\pi t)\sin m\nu$, that is,

$$a(t, \nu) = f(t, \nu)g(t, \nu) + t\sin\nu\sum_{n,m=1}^\infty a_{nm}\sin(n\pi t)\sin m\nu,$$

$$h(t, \nu) = vf(t, \nu) + \sin\nu\sum_{n,m=1}^\infty b_{nm}\sin(n\pi t)\sin m\nu. \tag{70}$$

Similarly, $h_1(t, \nu) - v$ vanishes when $t = 1$ and is finite when $t = 0$, $\nu = 0$, or $\nu = \pi$, so it can be expanded in the basis $(p, m \in \mathbb{Z})$,

$$\sin\left[\frac{p\pi}{2}(t + 1)\right]\sin m\nu, \qquad \sin\left[\frac{p\pi}{2}(t + 1)\right]\cos m\nu;$$

however, the conditions in (67c) select the latter basis elements, with $p = (2n + 1)$, $n \in \mathbb{Z}$. That is, we can expand

$$h_1(t, \nu) = v + c_0 k(t, \nu) + \sum_{n,m=0}^{\infty} c_{nm} \cos\left(\left(n + \frac{1}{2}\right)\pi t\right) \cos m\nu,$$

where we defined

$$k(t, \nu) = \frac{(\frac{Lgv}{2})^2 \sin^2 \nu}{t^2 (1 - t^2)^{-1} + (\frac{Lgv}{2})^2 \sin^2 \nu - \frac{1}{3}t^4}, \quad (71)$$

which is one between the quarks [$\nu \in (0, \pi)$, $t = 0$], thus allowing one to shift the value of $h_1$ there and zero on the other three edges. We note that terms with even $m$, in the expansions for $a$ and $h$, and with odd $m$, in the expansion for $h_1$, will always vanish due to reflection symmetry through the $(x_2, x_3)$ plane.

Finally, minimizing with respect to the first several Fourier coefficients, we obtained the profiles shown in Fig. 3. There, we can see $a$, $h$, $h_1$, and the energy density, in normal Cartesian coordinates $(z, \rho)$ (the mesh lines on the plotted surfaces are the elliptic coordinates used during the computations). In Fig. 3, we included the Fourier coefficients $a_{11}$, $a_{13}$, $a_{15}$, $a_{21}$, $a_{23}$, $a_{31}$, $b_{11}$, $b_{13}$, $b_{21}$, $c_0$, $c_{00}$, $c_{02}$, and $c_{10}$. Rerunning the minimization but only including $a_{11}$, $a_{13}$, and $a_{21}$ for $a$, keeping the previous $h$ and $h_1$ coefficients, the results are almost unchanged. Figure 4 displays (in percent) the relative errors defined as $2(a_{\text{more}} - a_{\text{few}})/(a_{\text{more}} + a_{\text{few}})$, with $a_{\text{more}}$ and $a_{\text{few}}$ the approximation to $a$ with more, respectively, fewer, Fourier coefficients (and analogously for $h$ and $h_1$). Applying these methods, we also obtained approximate solutions in $SU(3)$. In these initial computations, we included only the (1,1) mode in $a$ and $h$, and only the mode multiplying $k$ and the (0,0) mode for $h_0$, $h_1$, and $h_2$. The first two profiles, $a$ and $h$, are qualitatively similar to those obtained in $SU(2)$, while the last three are similar to $h_1$.

## V. A SPECIAL POINT IN PARAMETER SPACE

After developing appropriate numerical methods to solve the center string field equations, we have a tool that will permit us to contrast the model with existing lattice data. For this aim, we will also need some point in parameter space to start the search for the best fit. In this respect, we recall that in Ref. [26], the adjusted parameters in a dual Abelian Higgs model, when fitting the lattice interquark potential, turned out to be quite close to the BPS point. Moreover, in Ref. [28], the internal structure of the flux tube, within Abelian-projected $SU(2)$ lattice gauge theory, was reproduced by the dual Abelian lattice description. The masses of the dual gauge and Higgs fields turned out to be quite close, again a typical property associated with a BPS

point.[5] In both works, small deviations from this point favor a weakly type-I superconductor. However, these Abelian descriptions cannot explain the observed $N$-ality of confining strings. In this section, we will show how our effective model permits us to reconcile both properties.

### A. Center string BPS point

The $SU(2)$ center string profiles display a particular behavior when the mass parameter is varied. In Fig. 5, we display $a(\rho)$, $h(\rho)$, and $h_1(\rho)$, for $g = 0.1$, $\kappa = -2$, $\lambda = 1$, $v = 2.87$. The four cases correspond to $\mu = 0.8$, 0.6, 0.4, 0.2, respectively. We see that $h_1(\rho)$, the profile associated with the Higgs field along the Lie algebra constant direction $T_1$, tends to a constant function when $\mu \to 0$ (see Fig. 5). Indeed, at $\mu^2 = 0$, from Eq. (15), we have $v = -\kappa/\lambda$ ($\kappa < 0$), and it can be verified, not only for $SU(2)$ but also for $SU(3)$, that Eqs. (44) and (51) are satisfied by setting $h_1 \equiv v$ and $h_0 = h_1 = h_2 \equiv v$, independent of the form of $h$. That is, the field profiles for the Higgs fields that are not required to vanish on the $x^1$ axis become frozen at the asymptotic value $v$. In addition, the equations for the profile $h$, namely Eqs. (43) and (48), both become

$$\partial^2 h - \frac{(1 - a)^2}{(s_3)^2} h = (\lambda/2)h(h^2 - v^2). \quad (72)$$

This, together with Eq. (42), shows that, at $\mu^2 = 0$, $a$ and $h$ exactly satisfy the equations for Nielsen-Olesen vortices.

As the equations for the non-Abelian model get Abelianized, given that $\mu^2 = 0$, we may wonder whether the model (with $x^1$-translation symmetry) has a BPS point. This would permit us to discuss the stability of the fundamental vortex, showing these solutions correspond to energy minima with respect to *any* physical, possibly non-Abelian, change. A BPS bound in the bosonic sector of $\mathcal{N} = 2$ supersymmetric theory, based on a $U(N)$ gauge field, a complex adjoint, and $N$ fundamental scalars, was obtained in Ref. [31] (see also the review [61], and references therein). The BPS solutions include not only Abelian strings embedded in the non-Abelian description but also monopoles attached to a pair of strings.

For center strings, the initial steps we shall follow are similar to those given in Ref. [62], where we obtained a BPS point in a model based on the Lagrangian (12), (14), modified by the presence of a nonrelativistic term that tends to align $\psi_1$ and $B_1$ along the same direction in the Lie algebra. In that case, we used the condition $\mu^2 = \frac{2}{9}\frac{\kappa^2}{\lambda}$ [cf. Eq. (14)], where the Higgs potential becomes the perfect square in Eq. (13), and the decrease in energy due to the alignment term led all BPS solutions to have zero

---

[5]In $SU(3)$ a similar analysis points to a type-II superconductor [27].

(a) $a$



(b) $h$



(c) $h_1$



(d) subtracted energy density



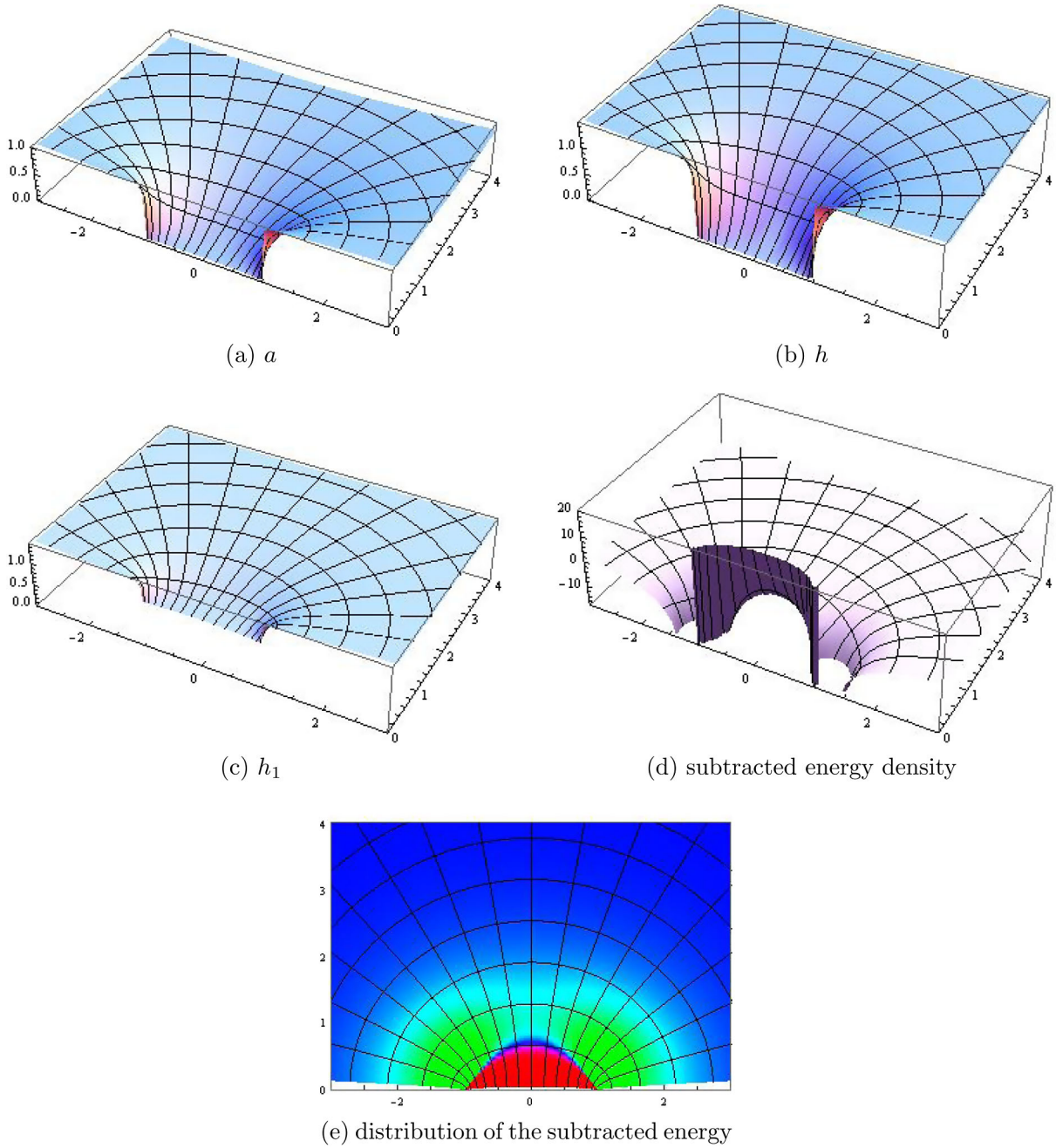(e) distribution of the subtracted energy

FIG. 3.   [$SU(2)$, $L = 2$, $g = 0.1$, $\mu = 0.9$, $\kappa = -2$, $\lambda = 1$, $v = 1.47$.] Here, we show the approximation with more Fourier coefficients described in the text. The axes are $x_1$, the radial distance to the $x_1$ axis, and the different profiles. The mesh corresponds to the prolate spheroidal coordinates used in the computations. (d) The energy density, after the quark self-energy density inside the integral in (68) has been subtracted. (e) Its spatial distribution.

energy. Here, we shall consider $\mu^2 = 0$ instead. In this case, after a general parametrization of the field color structure, the Higgs potential can also be written as a perfect square, leading to a relativistic model that accepts a BPS bound. This time, the minimum energy center string states will be $2\pi v^2$ and 0, for fundamental and adjoint charges, respectively.

Let us consider infinite center strings in $SU(2)$ and the complexified variable,

$$\zeta = \frac{\psi_2 + i\psi_3}{\sqrt{2}}, \quad \psi_2 = \frac{\zeta + \zeta^\dagger}{\sqrt{2}}, \quad \psi_3 = \frac{\zeta - \zeta^\dagger}{\sqrt{2}i}. \quad (73)$$

In this section, we use Cartesian coordinates and assume translation symmetry along the $x^1$ axis. Then, using the cyclicity property,

$$\langle X, [Y, Z] \rangle = \langle [X, Z^\dagger], Y \rangle, \quad (74)$$

(a) relative error on $a$



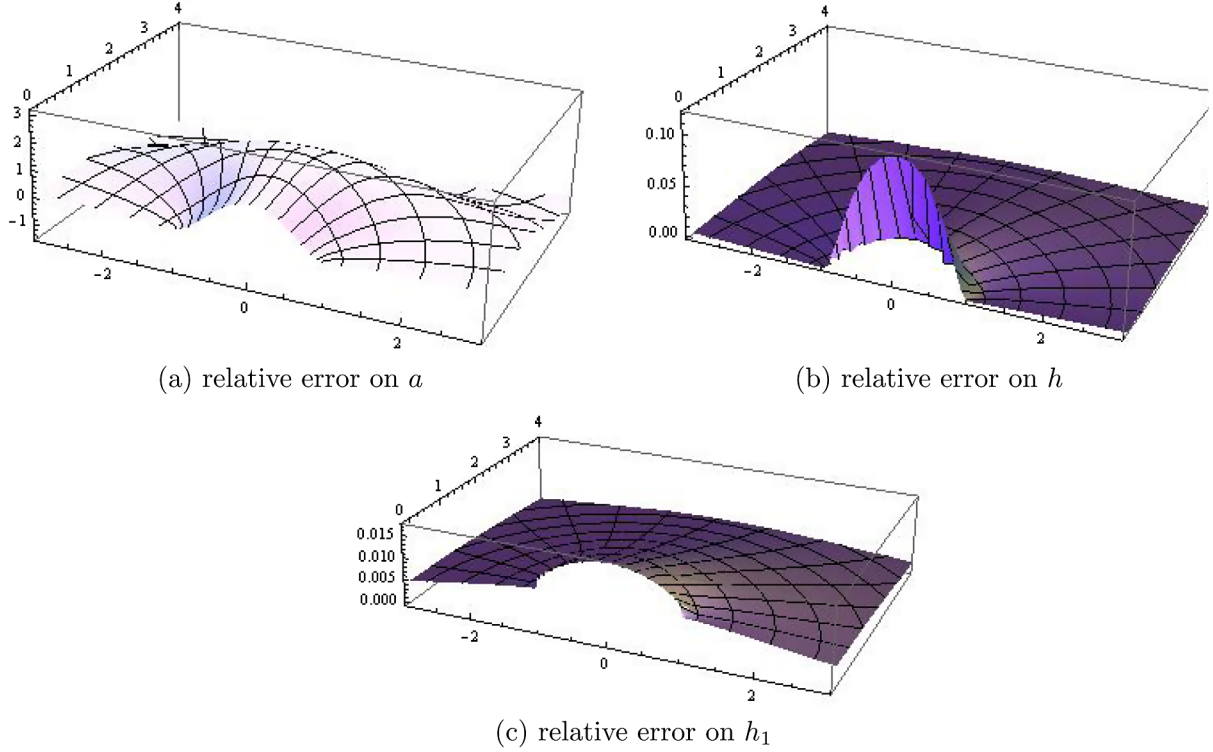(b) relative error on $h$



(c) relative error on $h_1$

FIG. 4. Relative errors, in percent, for the first three profiles in Fig. 3.

the hermiticity of $A_i$, and the Jacobi identity, we have ($i = 2, 3$)

$$\langle D_i X, D_i X \rangle = \langle DX, DX \rangle + g \langle B_1, [X, X^\dagger] \rangle + \partial_3 \langle X, iD_2 X \rangle - \partial_2 \langle X, iD_3 X \rangle, \quad (75)$$

where $D = D_2 + iD_3$. For example, taking $X = \zeta$, we obtain

$$\langle D_i \zeta \rangle^2 = \langle D\zeta \rangle^2 + g \langle [\zeta, \zeta^\dagger], B_1 \rangle + \partial_3 \langle \zeta, iD_2 \zeta \rangle - \partial_2 \langle \zeta, iD_3 \zeta \rangle, \quad (76)$$

and the energy per unit length becomes

$$\mathcal{E} = \int d^2 x \rho,$$

$$\rho = \frac{1}{2} \langle D_i \psi_1 \rangle^2 + \langle D\zeta \rangle^2 + \frac{1}{2} \langle B_1 \rangle^2 + g \langle [\zeta, \zeta^\dagger], B_1 \rangle + V_{\text{Higgs}}, \quad (77)$$

where we have used the boundary condition,

$$D_i \zeta \to 0 \quad \text{for } (x^2, x^3) \to \infty, \quad (78)$$

needed for a finite $\mathcal{E}$. Now, in the general parametrization $\psi_A = \Psi|_{AB} T_B$, the $3 \times 3$ real matrix $\Psi$ can always be decomposed as the product of a lower triangular matrix $L$

times an orthogonal matrix. If $\Psi$ is invertible, requiring the diagonal elements of $L$ to be positive, the factorization is unique. As a matrix in $O(3)$ is a sign times an $SO(3)$ matrix, and $\det L = L_{11} L_{22} L_{33}$, when $\det \Psi > 0$ ($\det \Psi < 0$) there is a unique decomposition $\Psi = +LR^T$ ($\Psi = -LR^T$), with $R^T \in SO(3)$. That is, we can represent

$$\psi_1 = L_{11} n_1,$$
$$\psi_2 = L_{21} n_1 + L_{22} n_2,$$
$$\psi_3 = L_{31} n_1 + L_{32} n_2 + L_{33} n_3, \quad (79)$$

where $n_A = ST_A S^{-1} = T_B R_{BA}$. For $SU(2)$, in our conventions, we have $f_{123} = 1/\sqrt{2}$. Then, setting $\mu^2 = 0$, using the asymptotic vacuum value $v = -\kappa/\lambda$ ($\kappa < 0$), and $c = (1/4)\lambda v^4$, needed to have zero potential energy at the vacuum, the Higgs potential can be cast in the form

$$V_{\text{Higgs}} = \frac{\lambda}{4} [L_{11}^2 (L_{22} - L_{33})^2 + 2 L_{22} L_{33} (L_{11} - v)^2 + (L_{22} L_{33} - v^2)^2] + \frac{\lambda}{4} [(L_{11} L_{32})^2 + (L_{21} L_{33})^2 + (L_{21} L_{32} - L_{22} L_{31})^2]. \quad (80)$$

Finally, expanding

$$B_1 = B_{11} n_1 + B_{12} n_2 + B_{13} n_3, \quad (81)$$

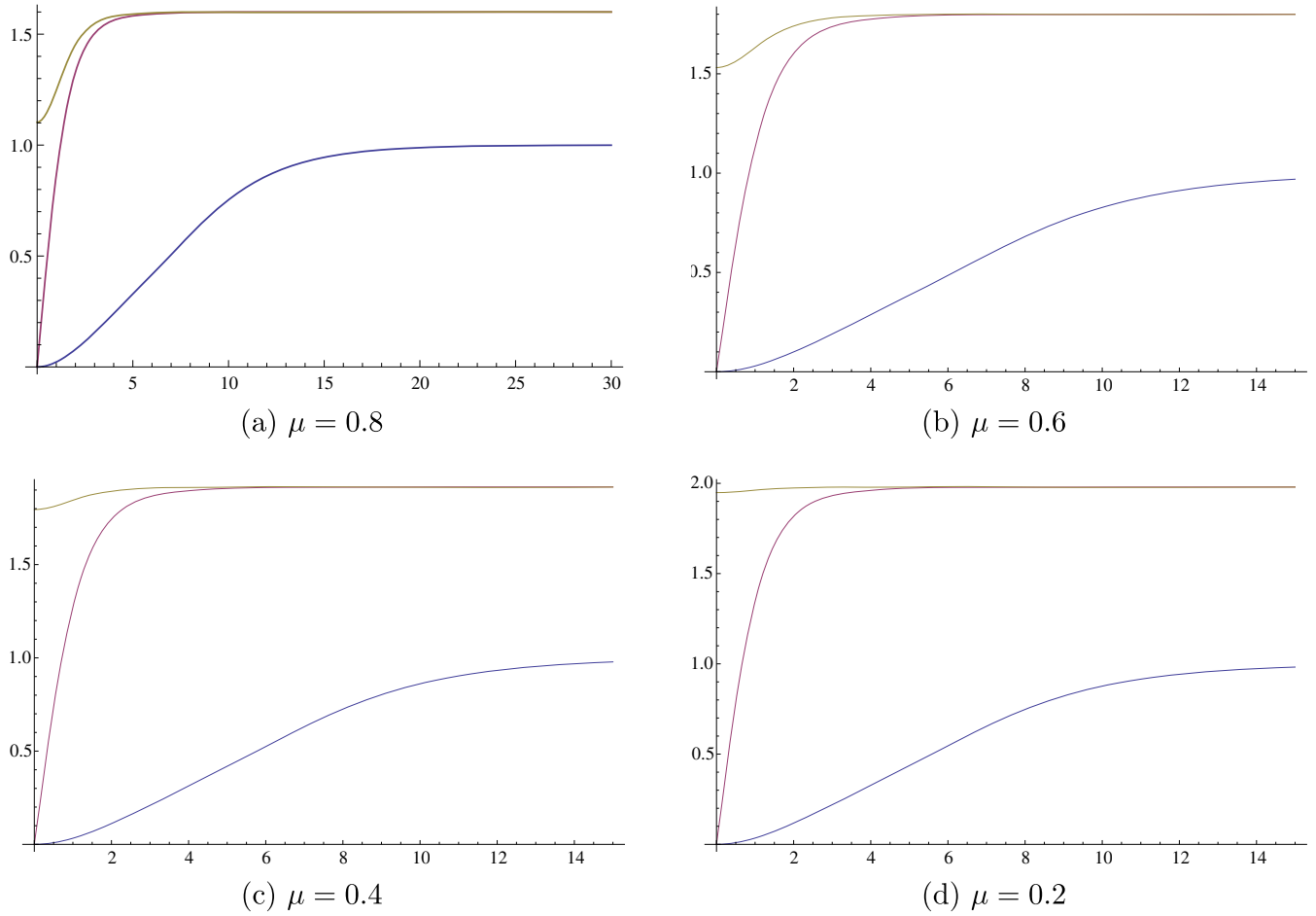(a) $\mu = 0.8$

(b) $\mu = 0.6$

(c) $\mu = 0.4$

(d) $\mu = 0.2$

FIG. 5.    $[SU(2), g = 0.1, \kappa = -2, \lambda = 1.]$ $a(\rho)$ (lower blue line), $h(\rho)$ (central red line), $h_1(\rho)$ (upper yellow-green line).

we note that at $\lambda = g^2$ we can write

$$
\rho = \frac{1}{2} \langle D_i \psi_1 \rangle^2 + \langle D\zeta \rangle^2 + \frac{1}{2} \left[ B_{11} + \frac{g}{\sqrt{2}} (L_{22} L_{33} - v^2) \right]^2
$$

$$
+ \frac{gv^2}{\sqrt{2}} B_{11} + \frac{1}{2} \left[ B_{12} - \frac{g}{\sqrt{2}} L_{21} L_{33} \right]^2
$$

$$
+ \frac{1}{2} \left[ B_{13} + \frac{g}{\sqrt{2}} (L_{21} L_{32} - L_{22} L_{31}) \right]^2
$$

$$
+ \frac{g^2}{4} [L_{11}^2 (L_{22} - L_{33})^2 + 2 L_{22} L_{33} (L_{11} - v)^2
$$

$$
+ (L_{11} L_{32})^2]. \tag{82}
$$

Setting the squares to zero, we get the BPS equations. Among them, $L_{11} = v$ and $D_i \psi_1 = 0$ lead to the condition $D_i n_1 = 0$. Using the fields $C_i^A$ defined in Eq. (17), the general solution to this condition is (see Ref. [22] and references therein)

$$
A_i = a_i n_1 - C_i^a n_a, \tag{83}
$$

$a = 2$, 3, and the resulting magnetic field is along $n_1$; that is, $B_{12} = 0$, $B_{13} = 0$,

$$
B_{11} = \partial_2 a_3 - \partial_3 a_2 - \frac{g}{2} \epsilon_{1jk} f^{1ab} C_j^a C_k^b. \tag{84}
$$

For a finite energy, the asymptotic behavior $a_i \to -C_i^1$ is required, as the combination $-C_i^A n_A$ is *locally* a pure gauge field. The associated field strength is

$$
F_{ij} = -F_{ij}^A(C) n_A, \quad F_{ij}^A(C) = \partial_i C_j^A - \partial_j C_i^A + g f^{ABC} C_i^B C_j^C.
$$

If $n_1$ is well defined everywhere, then the only nonzero component is $F_{ij}^1(C)$, and it is concentrated on the string where $n_2$, $n_3$ are ill defined, as occurs at the center string guiding center [cf. Eq. (26)]. Noting that

$$
\int d^2 x (\partial_2 a_3 - \partial_3 a_2) = \oint dx_i a_i = -\oint dx_i C_i^1
$$

$$
= \int d^2 x (\partial_2 C_3^1 - \partial_3 C_2^1),
$$

we obtain

$$\int d^2x B_{11} = -\frac{1}{2}\int d^2x \epsilon_{1jk} F_{jk}^1(C). \qquad (85)$$

Then, under the condition $D_i n_1 = 0$, the flux of $B_1$ projected along $n_1$ is topological and invariant under *regular* gauge transformations. For a single center string, this flux turns out to be $2\pi\sqrt{2}/g$ (see [22]), and the energy per unit length becomes $\mathcal{E} = 2\pi v^2$. Setting the remaining squares to zero gives

$$L_{22} = L_{33} = h, \qquad L_{21} = L_{31} = L_{32} = 0,$$
$$D\zeta = 0, \qquad B_{11} = \frac{g}{\sqrt{2}}(v^2 - h^2). \qquad (86)$$

Finally, using that $A_i$ is locally given by $S(a_i + C_i^1)T_1 S^{-1} + \frac{i}{g}S\partial_i S^{-1}$, we get

$$a_i = \frac{\sqrt{2}}{g}\epsilon_{ij}\partial_j \ln h - C_i^1,$$
$$-\partial^2 \ln h + 2\pi\delta^{(2)}(x_2, x_3) = \frac{g^2}{2}(v^2 - h^2). \qquad (87)$$

It is important to underline that the compatibility of the BPS and YMH equations is due to the fact that the energy density (82) is bounded by (a constant times) the projection $\langle n_1, B_1\rangle$, $\langle n_1\rangle^2 = 1$. This would not be the case if the projection were along the dynamical Higgs field $\psi_1$, as occurs at $\mu^2 = \frac{2}{9}\frac{\kappa^2}{\lambda}$, where it is necessary to redefine the model by subtracting a nonrelativistic term proportional to $\langle \psi_1, B_1\rangle$ [62]. A similar field-dependent projection is observed in the BPS center string bound of Ref. [32]. In that case, to keep the equations compatible, an appropriate limiting behavior of the parameters was needed.

As the BPS bound does not rely on cylindrical symmetry, we can conclude that there are no forces between fundamental center strings carrying the same weight and separated by a finite distance. This can easily be modified by moving around in parameter space. For other properties related with string interactions in $SU(N)$, see Secs. II B 1 and V C.

### B. N-ality

At the beginning of Sec. V, assuming cylindrical symmetry, Abelianized equations in $SU(2)$ and $SU(3)$ flavor symmetric models were obtained at $\mu^2 = 0$. More recently, an extension of this property to $SU(N)$ has also been derived, including an ansatz for $k$ strings[6] with weight given by $k$ times a fundamental weight [63]. As our model has an $SU(N) \to Z(N)$ SSB pattern, this Abelian-like

behavior coexists with $N$-ality. Take, for example, a pair of external adjoint quarks. The minimum energy solution will not be characterized by the Abelian-like phase in Eq. (19) but rather by a non-Abelian phase. In effect, let us consider the maps,

$$S_{\text{Abe}} = e^{i\varphi 2N\vec{\alpha}\cdot\vec{T}}, \qquad S_{\text{non-Abe}} = e^{i\varphi\vec{\beta}_1\cdot\vec{T}} e^{i\gamma\sqrt{N}T_\alpha} e^{-i\varphi\vec{\beta}_2\cdot\vec{T}}, \qquad (88)$$

where $\gamma \in [0, \pi]$ is the angle in a bipolar coordinate system, with foci at the quark locations, on any plane that contains the quarks. The fundamental weights $\vec{\beta}_i$ are chosen such that $\vec{\beta}_1 - \vec{\beta}_2 = 2N\vec{\alpha}$. On the $x^1$ axis, when $x^1 \in (-\infty, -L/2)$ or $(+L/2, +\infty)$, $\gamma$ vanishes and

$$S_{\text{non-Abe}} = e^{i\varphi(\vec{\beta}_1 - \vec{\beta}_2)\cdot\vec{T}}. \qquad (89)$$

On the other hand, between the quarks $\gamma = \pi$, so that there are no frame singularities in that region,

$$S_{\text{non-Abe}} \sim e^{i\pi\sqrt{N}T_\alpha}. \qquad (90)$$

In the Abelian case, the second term in the field strength tensor (18) has a nontrivial contribution,

$$-F_{23}^A(C)n_A = \frac{2\pi}{g}2N\vec{\alpha}\delta^{(2)}(x^2, x^3), \qquad (91)$$

while in the non-Abelian case, this contribution is

$$-F_{23}^A(C)n_A = \frac{2\pi}{g}2N\vec{\alpha}\delta^{(2)}(x^2, x^3)[\theta(x^1 - L/2) + \theta(-x^1 - L/2)] = J_{ij}, \qquad (92)$$

where $\theta(\cdot)$ is the Heaviside step function. Then, at points with $|x^1| > L/2$ on the $x^1$ axis, taking the condition $\mathcal{A}_\mu^A \to 0$, in both cases the external Dirac string $J_{ij}$ for adjoint quarks is canceled. The difference is that, in the Abelian case, to get a smooth energy density (22) at points with $|x^1| < L/2$ on the $x^1$ axis, the condition $\mathcal{A}_\mu^A \to \mathcal{C}_\mu^A$ is needed, and profiles associated with off-diagonal generators rotated by $S_{\text{Abe}}$ should go to zero. On the other hand, in that region, in the non-Abelian case, a smooth energy density is compatible with the condition $\mathcal{A}_\mu^A \to 0$ and, because of Eq. (90), no special regularity condition for the Higgs field profiles is needed. Then, using the Abelian or the non-Abelian phase, the energy minimization will return a positive or zero value, respectively. This corresponds to an excited adjoint string (local minimum) or the absence of a confining string between adjoint quarks (global minimum).

---

[6]They can be found for $N \geq 4$.

## C. Perspectives

Although a BPS bound for $N \geq 3$ has not been derived yet, it is clear that $\mu^2 = 0$, $\lambda = g^2$, is a good point to start exploring the parameter space and accommodate the field transverse localization lengths in confining strings; at this point, the magnetic and Higgs field localization lengths coincide. Another important piece of information to be accommodated was obtained in $SU(N)$ lattice YM theory ($N \geq 4$) [30]. In particular, the ratios of $k$ string to fundamental string tensions are compatible with either a sine law, $\sigma_k / \sigma_f = \sin \frac{k\pi}{N} / \sin \frac{\pi}{N}$, or a Casimir law, $\sigma_k / \sigma_f = k(N-k)/(N-1)$. In both cases $\sigma_2 < 2\sigma_f$, so it is expected that the interaction between center strings with the same fundamental weight is attractive. For large $N$, and finite $k$, the ratios become linear, thus signaling they become noninteracting in this limit. Starting at $\mu^2 = 0$, $\lambda = g^2$, attractive or repulsive interactions can be obtained by changing the model parameters. For example, keeping $\mu^2 = 0$ and moving to $\lambda < g^2$, $k$ strings are expected to be bound states of $k$ fundamental strings. Studies about how the above-mentioned properties depend on $\mu^2$, which in the SSB region can go from negative values up to $\mu^2 < \frac{2}{9}\frac{\kappa^2}{\lambda}$, the fitting to sine or Casimir laws, as well as the interquark potentials are in progress [63].

In particular, the comparison with lattice potentials will be facilitated by the use of scaled variables,

$$L = x/\sqrt{\sigma}, \qquad f(x) = (1/\sqrt{\sigma})V(x/\sqrt{\sigma}), \quad (93)$$

where $\sigma$ is the string tension, a natural scale in the problem, which contains a pair of parameters with dimension of mass, $\mu$, $\kappa$ (and a pair of adimensional ones $g$, $\lambda$). The tension can be computed following the methods in Sec. IV A, for given input parameters, and it can be fixed to be $\sigma = (440 \text{ MeV})^2$. For instance, the $SU(2)$ lattice potential was adjusted by

$$V(L) \approx c - e/L + \sigma L, \quad (94)$$

with $e \sim 0.256$ (see Refs. [59,64]). This, together with the BPS properties, can give an idea about typical input parameters. At smaller distances our potential should be Coulomb-like $\sim -\frac{Q_m^2}{4\pi L}$ where $Q_m$ is the monopole charge representing the fundamental quark. In our conventions, the charge for a fundamental monopole is $Q_m = \frac{2\pi}{g}\sqrt{2}$. At $\mu = 0$, where the equations get Abelianized, the vacuum value is $v = -\kappa/\lambda$, and at $\lambda = g^2$ the string tension is $\sigma = 2\pi v^2$. Thus, merging all this information, typical values are obtained from

$$g = \sqrt{\frac{2\pi}{e}}, \qquad \mu = 0, \qquad \kappa = -\frac{\sqrt{2\pi\sigma}}{e}, \qquad \lambda = \frac{2\pi}{e}, \tag{95}$$

which implies

$$g = 5.01, \qquad \mu = 0,$$
$$v = -\kappa/\lambda = 175.55 \text{ (in MeV)}, \qquad \lambda = 25.13. \quad (96)$$

Finally, we note that the stringlike behavior is expected for interquark separations much larger than both the magnetic and the Higgs field localization widths, given by $\sim 1/(gv)$ and $\sim 1/(\sqrt{\lambda}v)$, respectively. However, it is interesting to note that lattice calculations point to a static potential that is well described by Eq. (94) over a large range of $L$ values, from asymptotic to smaller distances where the flux tube picture is no longer valid. That is, although the origin of the $1/L$ effects at small and large distances are different, both regimes are described by a single $1/L$ term.[7] This type of "continuous" behavior was also noted for $SU(N)$ in Ref. [60] and could indicate that the validity of the model could also be extended. In this respect, it would also be interesting to analyze the hybrid states and the effect of the adjoint dual monopole (valence gluon) on the hybrid potential.

## VI. CONCLUSIONS

The detailed knowledge we have about interquark lattice potentials makes us wonder what the natural effective description for the Yang-Mills vacuum could be. This search can be guided by the symmetries, by the way they are realized, by the identification of large distance relevant terms in the functional energy, and, of course, by the lattice data. Here, we analyzed a natural class of models with $SU(N) \to Z(N)$ SSB. This is an interesting SSB pattern, as the confining string would incorporate $N$-ality. Initially, we tested a numerical method to solve the center string field equations, obtaining the solutions for infinite and finite center strings, the latter running between a monopole and an antimonopole, representing the external quark and antiquark, respectively.

In fact, the lattice interquark potential has already been adjusted in different phenomenological models, and the lattice data seem to set the parameters close to the interface between type I and type II superconductors. For instance, this has been observed in a dual Abelian Higgs model that essentially describes a condensate of Abelian monopoles. However, we know that in that case, $N$-ality cannot be accommodated. In the second part of this work, we reconciled both properties in our framework. We showed numerically and analytically [for $SU(2)$ and $SU(3)$] that there is a region in parameter space where the field equations freeze some Higgs profiles to a constant vacuum value. In this region, the profiles for the gauge field along a local Cartan direction, and for the Higgs fields that rotate,

---

[7]The lattice coefficient $e \sim 0.256$, obtained by including smaller separations, turns out to match the Lüscher value $\pi/12$.

exactly satisfy Nielsen-Olesen equations. So we can already conclude that in our non-Abelian context, the fitting of lattice data will be as good as in the Abelian one, with the advantage of implementing $N$-ality.

Moreover, in the case of $SU(2)$, after freezing one of the Higgs fields at a local vacuum value, we derived a BPS bound that is topological and gauge invariant under regular gauge transformations. This point provides the type-I/type-II superconductor interface. The steps followed are similar to those previously given to derive a BPS point, at $\mu^2 = \frac{2}{9}\frac{\kappa^2}{\lambda}$, $\lambda = g^2$, by the inclusion of a nonrelativistic interaction that tends to align the magnetic field and one of the Higgs fields along the same Lie algebra direction. As a consequence, in that work, all BPS solutions had zero energy. Here, we have shown that to get a BPS bound at $\mu^2 = 0$, $\lambda = g^2$, the model requires no alignment term. This time, the minimum energy center string states are $2\pi v^2$ and 0, for fundamental and adjoint charges, respectively.

These are essential tools that will permit one to determine, in a forthcoming work, the appropriate model that is compatible with the various observables already computed in the lattice, as normal and hybrid potentials, and the energy density profiles.

## ACKNOWLEDGMENTS

[1] G. S. Bali, Phys. Rep. **343,** 1 (2001).
[2] M. Lüscher and P. Weisz, J. High Energy Phys. 07 (2002) 049.
[3] S. Kratochvila and P. de Forcrand, Nucl. Phys. **B671,** 103 (2003).
[4] Y. Nambu, Phys. Rev. D **10,** 4262 (1974).
[5] S. Mandelstam, Phys. Rep. **23C,** 245 (1976).
[6] G. 't Hooft, Nucl. Phys. **B138,** 1 (1978).
[7] G. S. Bali, V. Bornyakov, M. Muller-Preussker, and K. Schilling, Phys. Rev. D **54,** 2863 (1996).
[8] J. Greensite, K. Langfeld, S. Olejnik, H. Reinhardt, and T. Tok, Phys. Rev. D **75,** 034501 (2007).
[9] M. Faber, J. Greensite, and S. Olejnik, Phys. Rev. D **57,** 2603 (1998).
[10] M. Engelhardt and H. Reinhardt, Nucl. Phys. **B567,** 249 (2000).
[11] J. M. Cornwall and B. Yan, Phys. Rev. D **53,** 4638 (1996).
[12] L. Del Debbio, M. Faber, J. Greensite, and S. Olejnik, Phys. Rev. D **55,** 2298 (1997).
[13] K. Langfeld, H. Reinhardt, and O. Tennert, Phys. Lett. B **419,** 317 (1998); **431,** 141 (1998).
[14] Ph. de Forcrand and M. Pepe, Nucl. Phys. **B598,** 557 (2001).
[15] F. V. Gubarev, A. V. Kovalenko, M. I. Polikarpov, S. N. Syritsyna, and V. I. Zakharov, Phys. Lett. B **574,** 136 (2003).
[16] G. Mack and V. B. Petkova, Ann. Phys. (N.Y.) **123,** 442 (1979); **125,** 117 (1980).
[17] M. Baker, J. S. Ball, and F. Zachariasen, Phys. Rev. D **41,** 2612 (1990).
[18] M. Baker, J. S. Ball, and F. Zachariasen, Phys. Rev. D **44,** 3328 (1991).
[19] A. Gorsky, M. Shifman, and A. Yung, Phys. Rev. D **71,** 045010 (2005).
[20] K. Konishi, Lect. Notes Phys. **737,** 471 (2008).
[21] K. Konishi and L. Spanu, Int. J. Mod. Phys. A **18,** 249 (2003).
[22] L. E. Oxman, J. High Energy Phys. 03 (2013) 038.

[23] M. Baker, J. S. Ball, and F. Zachariasen, Phys. Rev. D **51,** 1968 (1995).
[24] M. Baker, J. S. Ball, and F. Zachariasen, Phys. Rev. D **56,** 4400 (1997).
[25] M. Baker, N. Brambilla, H. G. Dosch, and A. Vairo, Phys. Rev. D **58,** 034010 (1998).
[26] S. Maedan, Y. Matsubara, and T. Suzuki, Prog. Theor. Phys. **84,** 130 (1990).
[27] Y. Koma, E. M. Ilgenfritz, H. Toki, and T. Suzuki, Phys. Rev. D **64,** 011501(R) (2001).
[28] Y. Koma, M. Koma, E. M. Ilgenfritz, and T. Suzuki, Phys. Rev. D **68,** 114504 (2003).
[29] A. M. Green, C. Michael, and P. S. Spencer, Phys. Rev. D **55,** 1216 (1997).
[30] B. Lucini and M. Teper, Phys. Lett. B **501,** 128 (2001).
[31] D. Tong, Phys. Rev. D **69,** 065003 (2004).
[32] M. A. C. Kneipp and P. Brockill, Phys. Rev. D **64,** 125012 (2001).
[33] J. Greensite, Prog. Part. Nucl. Phys. **51,** 1 (2003).
[34] J. Greensite, *An Introduction to the Confinement Problem* (Springer, Berlin-Heidelberg, 2011).
[35] H. Reinhardt, Nucl. Phys. **B628,** 133 (2002).
[36] M. Engelhardt, M. Quandt, and H. Reinhardt, Nucl. Phys. **B685,** 227 (2004).
[37] K. Bardakci and S. Samuel, Phys. Rev. D **18,** 2849 (1978).
[38] M. Kiometzis, H. Kleinert, and A. M. J. Schakel, Fortschr. Phys. **43,** 697 (1995).
[39] H. Kleinert, *Path Integrals in Quantum Mechanics, Statistics, Polymer Physics, and Financial Markets* (World Scientific, Singapore, 2006).
[40] M. B. Halpern and W. Siegel, Phys. Rev. D **16,** 2486 (1977).
[41] D. Antonov, Surveys High Energy Phys. **14,** 265 (2000).
[42] L. E. Oxman, G. C. Santos Rosa, and B. F. I. Teixeira, J. Phys. A **47,** 305401 (2014).
[43] A. P. Balachandran, P. Salomonson, B. Skagerstam, and J. Winnberg, Phys. Rev. D **15,** 2308 (1977).

[44] L. E. Oxman (to be published).
[45] G. H. Fredrickson, *The Equilibrium Theory of Inhomogeneous Polymers*, 1st ed. (Clarendon Press, Oxford, 2006), p. 452.
[46] H. J. de Vega and F. A. Schaposnik, Phys. Rev. D **34**, 3206 (1986).
[47] H. J. de Vega, Phys. Rev. D **18**, 2932 (1978).
[48] H. J. de Vega and F. A. Schaposnik, Phys. Rev. Lett. **56**, 2564 (1986).
[49] J. Heo and T. Vachaspati, Phys. Rev. D **58**, 065011 (1998).
[50] L. E. Oxman, J. High Energy Phys. 07 (2011) 078.
[51] B. Ketzer, *Proc. Sci.*, QNP2012 (2012) 025.
[52] K. J. Juge, J. Kuti, and C. J. Morningstar, Nucl. Phys. B, Proc. Suppl. **63**, 326 (1998).
[53] L. E. Oxman, arXiv:1506.05186.
[54] A. Hanany and D. Tong, J. High Energy Phys. 07 (2003) 037.
[55] R. Auzzi, S. Bolognesi, J. Evslin, K. Konishi, and A. Yung, Nucl. Phys. **B673**, 187 (2003).
[56] A. Armoni and M. Shifman, Nucl. Phys. **B671**, 67 (2003).

[57] M. Shifman and A. Yung, Phys. Rev. D **77**, 066008 (2008).
[58] S. Monin, M. Shifman, and A. Yung, Phys. Rev. D **92**, 025011 (2015).
[59] G. S. Bali, C. Schlichter, and K. Schilling, Phys. Rev. D **51**, 5165 (1995).
[60] A. Athenodorou, B. Bringoltz, and M. Teper, *Proc. Sci.*, LAT2009 (2009) 223; M. Teper, Acta Phys. Pol. B **40**, 3249 (2009); A. Athenodorou, B. Bringoltz, and M. Teper, J. High Energy Phys. 02 (2011) 030.
[61] D. Tong, Ann. Phys. (Berlin) **324**, 30 (2009).
[62] L. E. Oxman, Adv. High Energy Phys. **2015**, 494931 (2015).
[63] G. Moreira Simões, L. E. Oxman, and D. Vercauteren (to be published); R. Höllwieser, L. E. Oxman, and D. Vercauteren (to be published).
[64] G. S. Bali, K. Schilling, and A. Wachter, Phys. Rev. D **55**, 5309 (1997).